

MATURE: Biogeochemistry of the Maximum TURbidity zone in Estuaries. A summary report.

Peter.M.J. Herman and Carlo Heip

Netherlands Institute of Ecology, Centre for Estuarine and Coastal Ecology, Vierstraat 28, 4401 EA Yerseke, The Netherlands.

211367

1. Introduction.

1.a. Aims and objectives.

The EU-environment research programme MATURE (Biogeochemistry of the MAXimum TURbidity zone in Estuaries) was a cooperation project between the following partners:

- NIOO, Yerseke (coordinator)
- University of Hamburg, Dept. of Marine Chemistry and Biogeochemistry
- University of Hamburg, Center of Marine and Climate Research
- NIOZ, Texel
- TNO, Den Helder
- University of Brussels
- University of Gent
- University of Bordeaux, station of Arcachon
- Instituto Tecnico Superior, Lisbon

The objectives of the programme are summarized as follows:

The role of biological processes in the formation and subsequent utilization of particles in the maximum turbidity zone will be studied in three European estuaries : Gironde, Schelde and Elbe. Special attention will be given to organic matter and biological processes acting on it. Nutrients and trace elements will be considered insofar as they are regulating biological processes in the estuary. Numerical modelling of water and suspended matter transport is an integrated part of the project.

Specific research questions addressed in the project are:

- How is the concentration, stability and fate of aggregates influenced by the transformations of organic matter, advected from river and human sources?
- How can formation, sedimentation and resuspension of particles be parameterized and incorporated into numerical hydrodynamic models?
- What is the importance of microbiological processes (primary production, bacterial mineralization, protozoan grazing) for the geochemistry of the system; what are the specific characteristics of the microbial loop on the aggregates; how do they affect the dynamics of the aggregates?
- How do the biological processes at higher trophic levels (selective grazing and manipulation of particles in the water column and upper layers of the sediment) affect the particle dynamics. Reversely, what is the influence of the geochemical environment on these processes?

1.b. Organization of the project.

The field work for the project has been centred around six joint field campaigns of appr. 1 week. In Spring 1993 and in Spring 1994 a one-week campaign has been organized in Elbe, Schelde and Gironde. A great number of physical, chemical, microbiological and macrobi-

ological measurements have been performed on common stations during these campaigns. Each of the campaigns started with an along-estuary transect, followed by a 24h cycle with hourly measurements at a fixed station, and by a second transect along the estuary. Sampling on the common stations was usually concentrated on surface, middle water and bottom water levels, although not all variables have always been determined at all the levels. CTD casts provided a better vertical resolution for a number of physical and chemical variables.

After analysis in the laboratory, all results have been gathered at NIOO and have been stored in a common database. This database ([Herman & de Hoop, this report](#)) with a manual and documentation, has been distributed among the partners of the project. In principle, it is freely available to the scientific community upon completion of the project.

Alongside the field measurements, laboratory experiments have been performed on specific biological questions, e.g. relating to the feeding biology of the zooplankton, and a mesocosm setup has been designed for experimental study of environmental stress on estuarine zooplankton communities.

Finally, 3D hydrodynamic models have been developed for the three estuaries. These models have been calibrated on available field and monitoring data. Their application to the analysis of the biogeochemical field data is not completed, however.

This scientific summary report highlights the conclusions that can be drawn from the interdisciplinary comparison of the results obtained. For a detailed description of the results of the different research groups, we refer to the reports of the partners given in appendix. A complete overview of these reports is given at the end of this summary.

2. Description of the MTZ during the field campaigns.

CTD profiles were obtained by the University of Hamburg (see Pfeiffer, this report) at many stations in and around the MTZ of the estuaries during the field campaigns. Two profiles along the estuary were sampled with a spatial resolution of around 10 km; during the 24h stations appr. every hour a CTD cast was made.

→ Results of the CTD casts are delivered by the University of Hamburg in a number of ASCII files. This partner provided a program to draw vertical profiles of the measured variables at every station (see Pfeiffer, this report). Results were combined in a Paradox data base containing all observations. From this database synoptic pictures were produced that summarize the data on salinity and light transmission (as a measure of turbidity) in this report. The CTD database is kept apart from the general biogeochemical database. It is included with the database as the files CTD.db (basic data) and CTDSTAT.DB (station data, linked to CTD.DB through the field "Station").

The light transmission values gave clear pictures of the vertical and horizontal distribution of suspended solids along the estuarine salinity gradients. Figs. 1-11 summarize salinity (upper picture, a) and light transmission (lower picture, b) in the Elbe in 1993 and 1994, Gironde 1993 and 1994 and Schelde 1993 and 1994. With one exception (Schelde 1993, where gradients of light transmission were hardly visible) there are clear gradients in suspended solids along the estuarine axis. Vertical gradients in light transmission were clearly visible and most pronounced where the average transmission was lower than appr. 60 %.

Fig. 12 shows the dependence of depth-averaged light transmission on salinity in the three estuaries and the two years. The relation of light transmission with salinity is closer than with position along the axis of the estuary (compare, e.g., the two transects in the Schelde in 1994: figs 10 and 11), indicating that the zone of maximum turbidity moves up and down the estuary with the tide.

In Gironde and Elbe, peak turbidity values are found at salinities between 0.1 and 4 psu. Turbidity in the Gironde is so high that transmissometry lacks enough resolution at the highest turbidity values. The situation in the Schelde seems to differ from the other two estuaries. In 1993 no clear maximum turbidity zone could be detected; in 1994 a peak value was found at a slightly higher salinity (peak at 4 psu, distinctly lower turbidity in the range 0.1-3). Despite the difference in river discharge rates between 1993 and 1994, causing the salinity gradient to be moved further downstream in all three estuaries (figs 1-11), there were no large differences in the relation of transmission with salinity between the two years in Elbe and Gironde. For the Schelde, again, the picture is less clear due to the lack of a distinct MTZ in 1993.

From these results it can be concluded that the MTZ in, at least, Elbe and Gironde and possibly also in the Schelde, is positioned in the very low salinity range of the estuary. It moves up- and downstream with the tide, and shifts along the estuarine axis, together with the salinity gradient, at differing discharge rates. In the field samples the concentration of suspended material in a maximum turbidity zone is closely linked to the transition zone from zero to very low salinities. Even if salinity *per se* is not the direct cause of the concentration of the suspended matter, it is closely correlated with the factors causing the peak turbidity.

A full description of the biogeochemical variables in the MTZ during the field campaigns is given by Brockmann et al. (this report) and will not be repeated here. These authors discuss the differences between the estuaries with respect to nutrients, oxygen and organic loadings. They conclude that anthropogenic stress in the Gironde is far less pronounced than in the other two estuaries. Nitrification in the maximum turbidity zone is well expressed in Elbe and Schelde. Denitrification is important in the Schelde.

Elbe 1993 transect 1

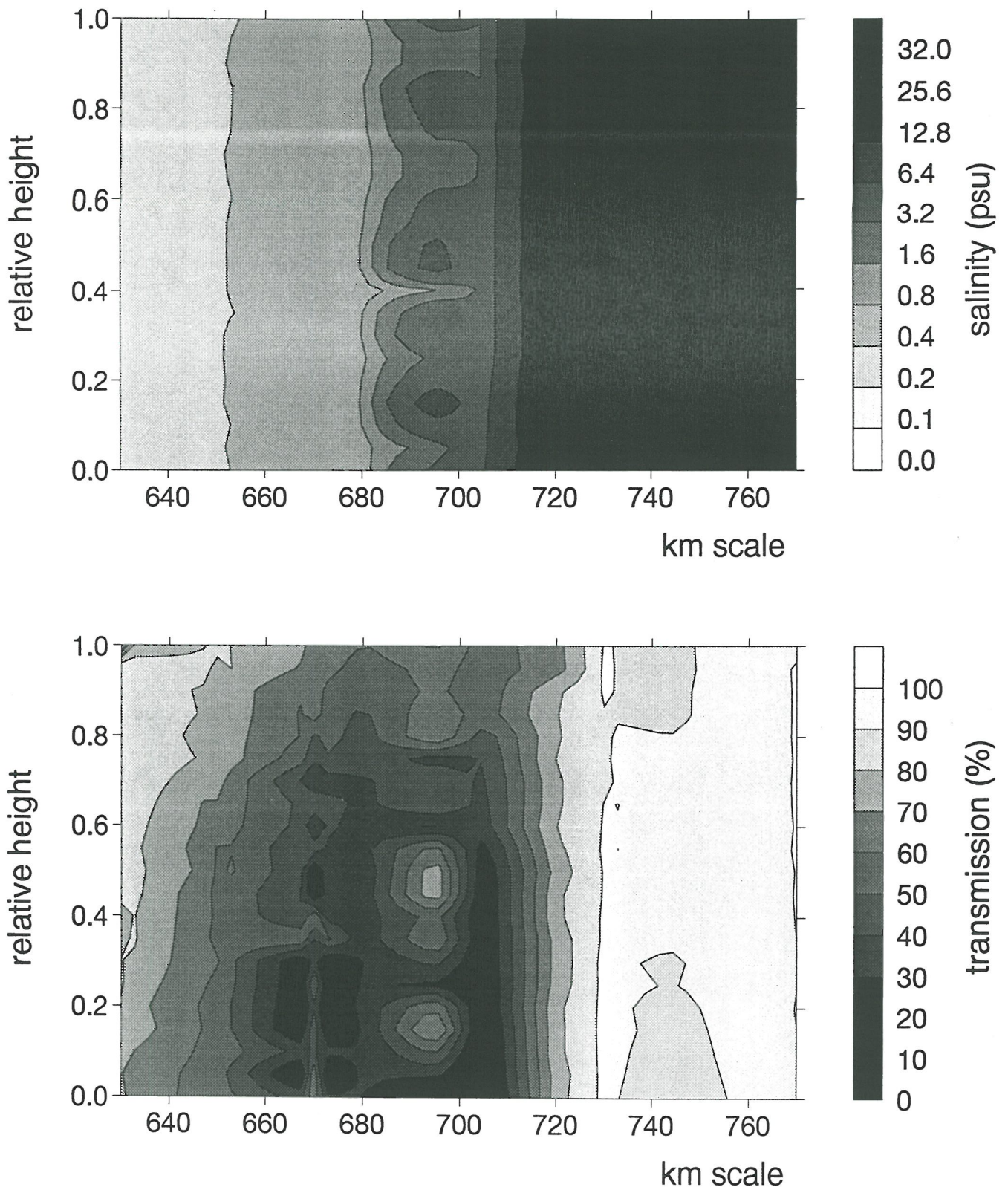


Fig. 1. (a) salinity and (b) light transmission profiles in the first transect, Elbe 1993. The horizontal scale is the longitudinal estuarine axis, the vertical scale is relative height above the bottom (1=surface, 0=bottom).

Elbe 1993 transect 2

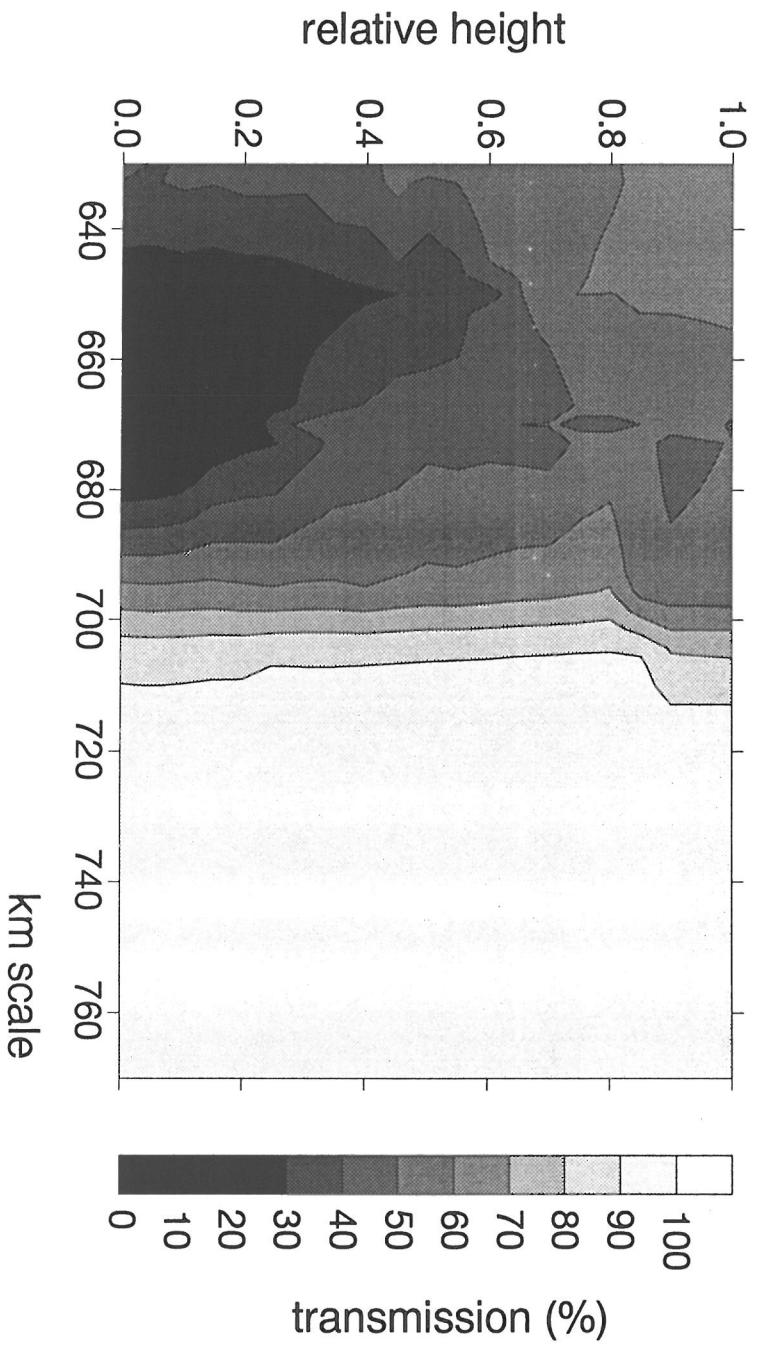
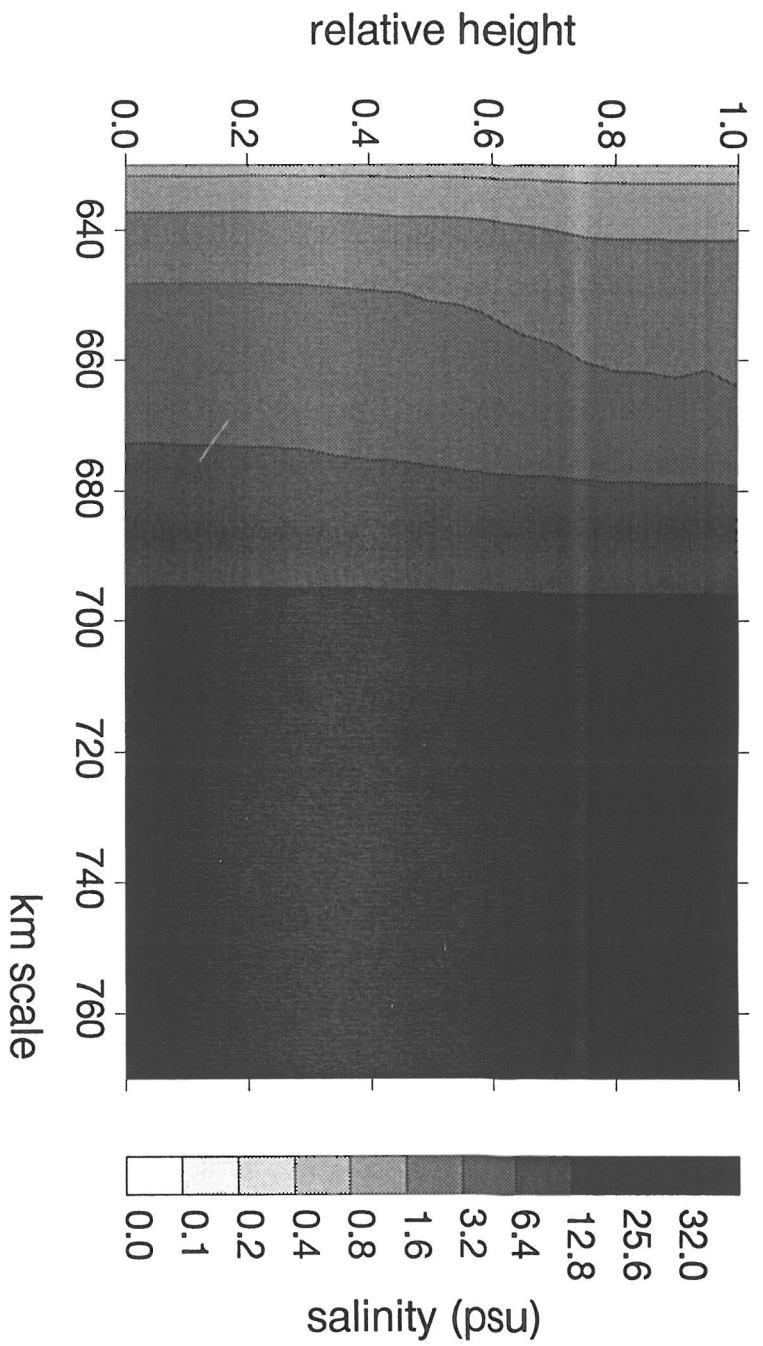


Fig. 2. (a) salinity and (b) light transmission profiles in the second transect, Elbe 1993. The horizontal scale is the longitudinal estuarine axis, the vertical scale is relative height above the bottom (1=surface, 0=bottom).

Elbe 1994 transect 1

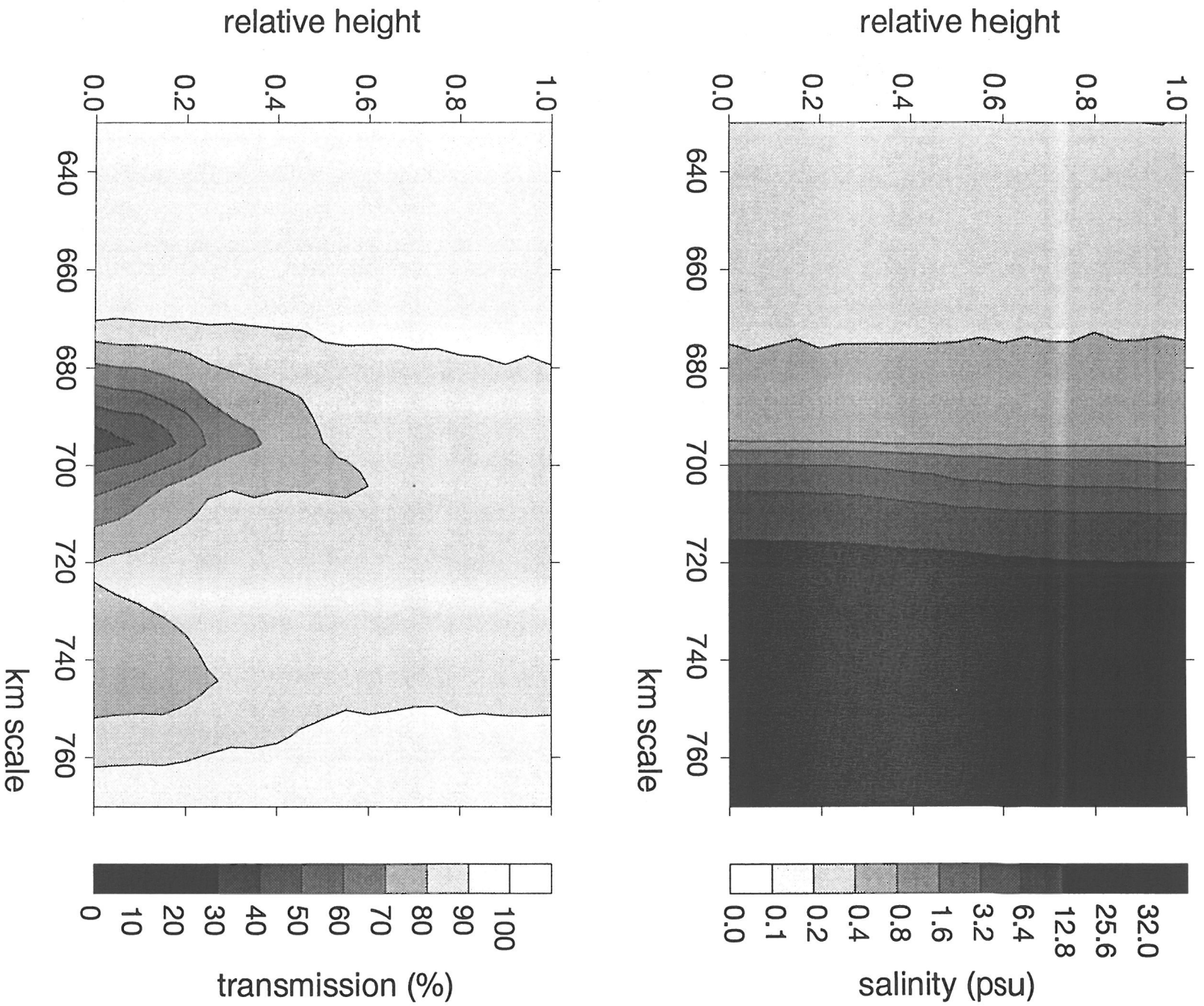


Fig. 3. (a) salinity and (b) light transmission profiles in the first transect, Elbe 1994. The horizontal scale is the longitudinal estuarine axis, the vertical scale is relative height above the bottom (1=surface, 0=bottom).

Elbe 1994 transect 2

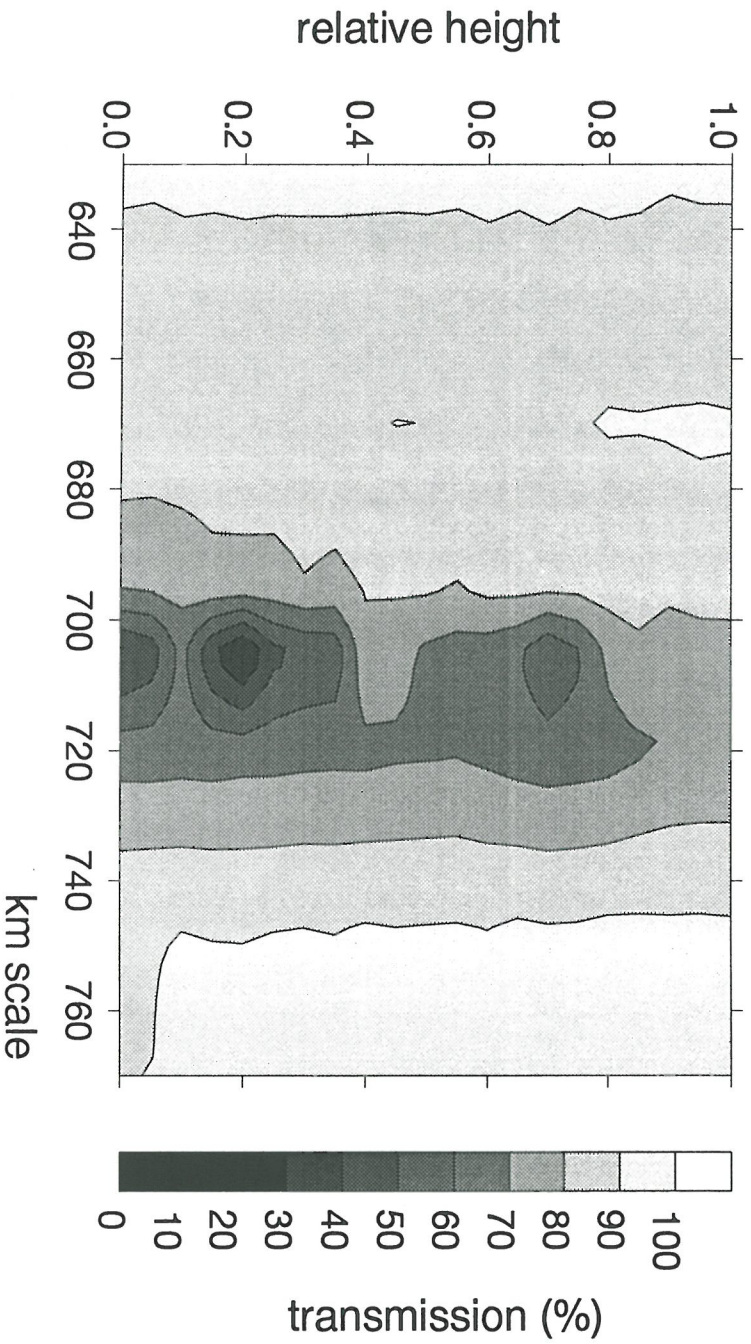
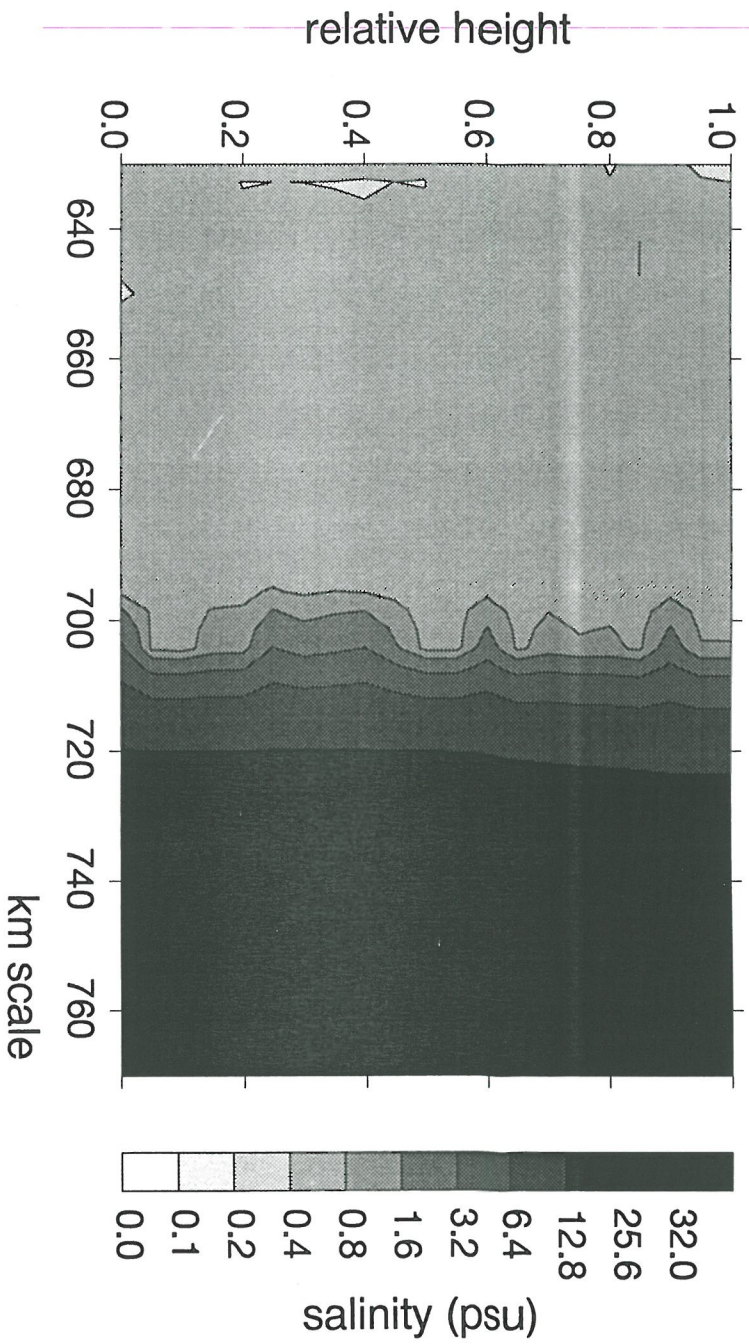


Fig. 4. (a) salinity and (b) light transmission profiles in the second transect, Elbe 1994. The horizontal scale is the longitudinal estuarine axis, the vertical scale is relative height above the bottom (1=surface, 0=bottom).

Gironde 1993 transect 1

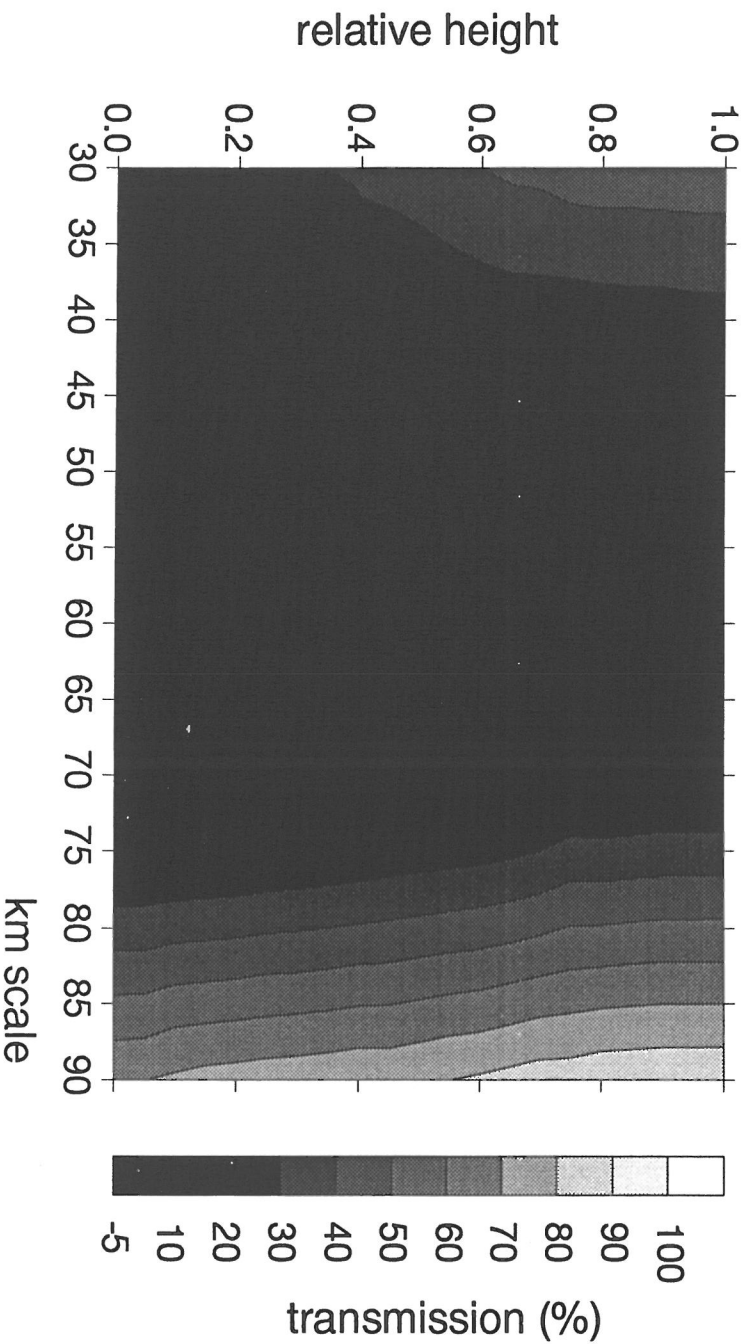
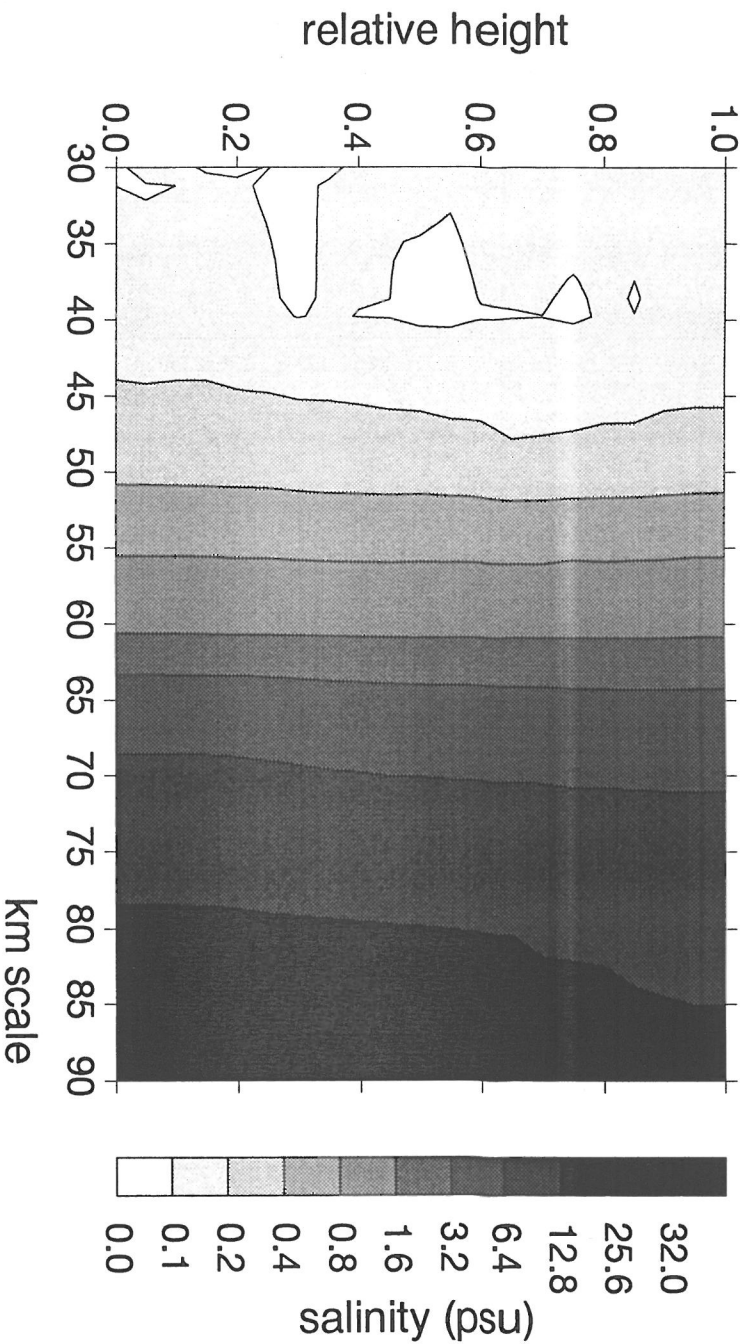


Fig. 5. (a) salinity and (b) light transmission profiles in the first transect, Gironde 1993. The horizontal scale is the longitudinal estuarine axis, the vertical scale is relative height above the bottom (1=surface, 0=bottom).

Gironde 1993 transect 2

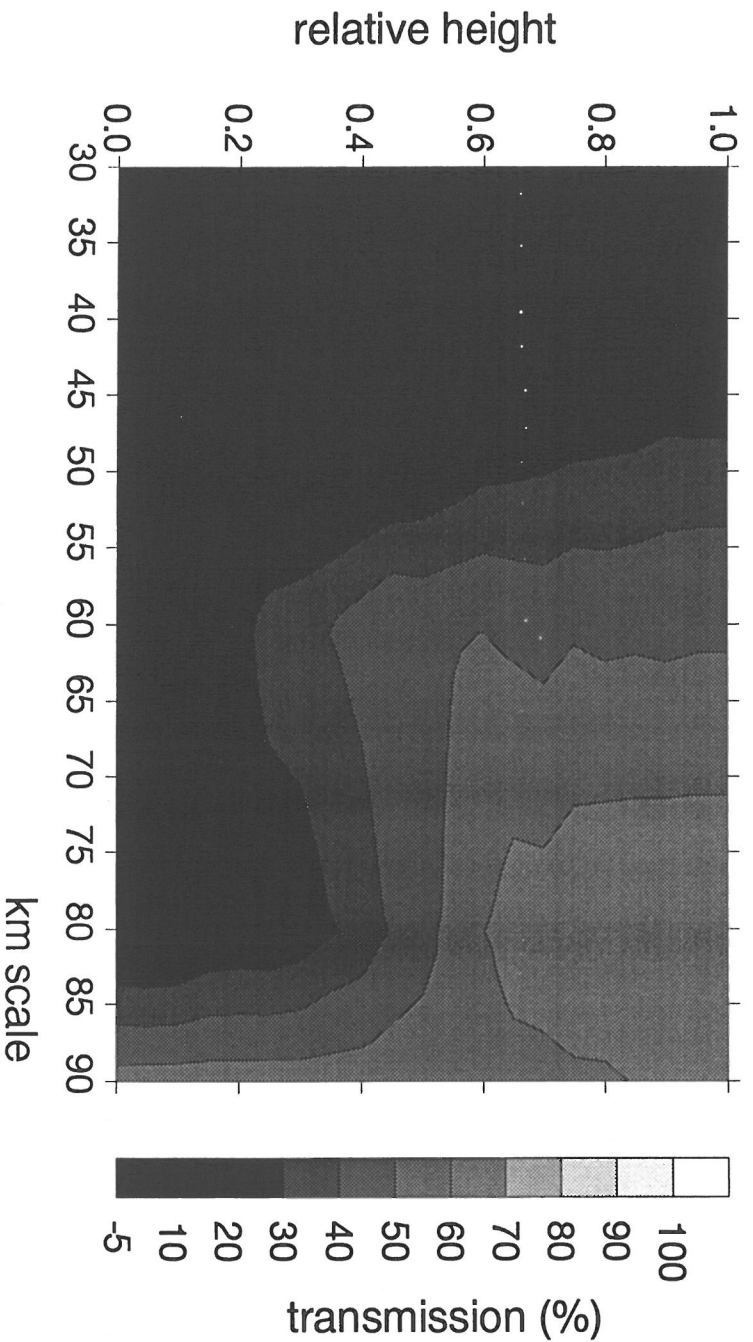
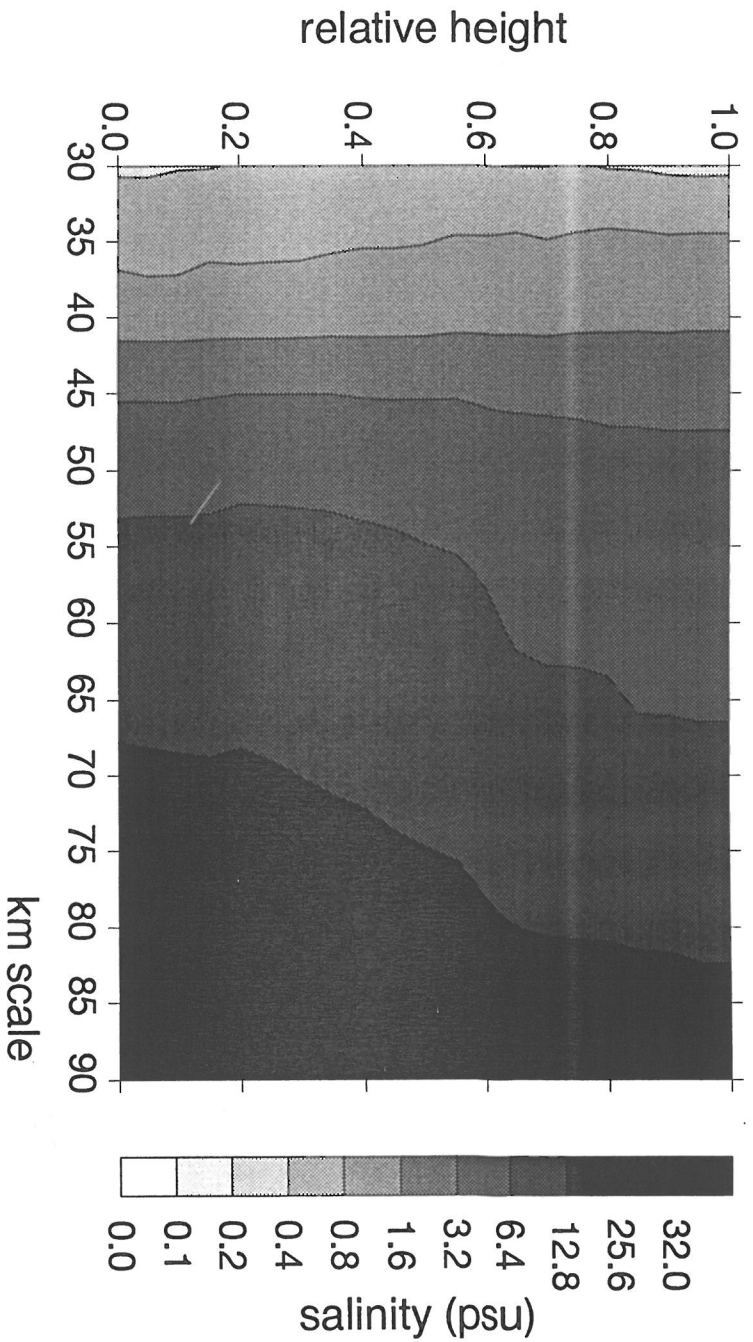


Fig. 6. (a) salinity and (b) light transmission profiles in the second transect, Gironde 1993. The horizontal scale is the longitudinal estuarine axis, the vertical scale is relative height above the bottom (1=surface, 0=bottom).

Gironde 1994 transect 1

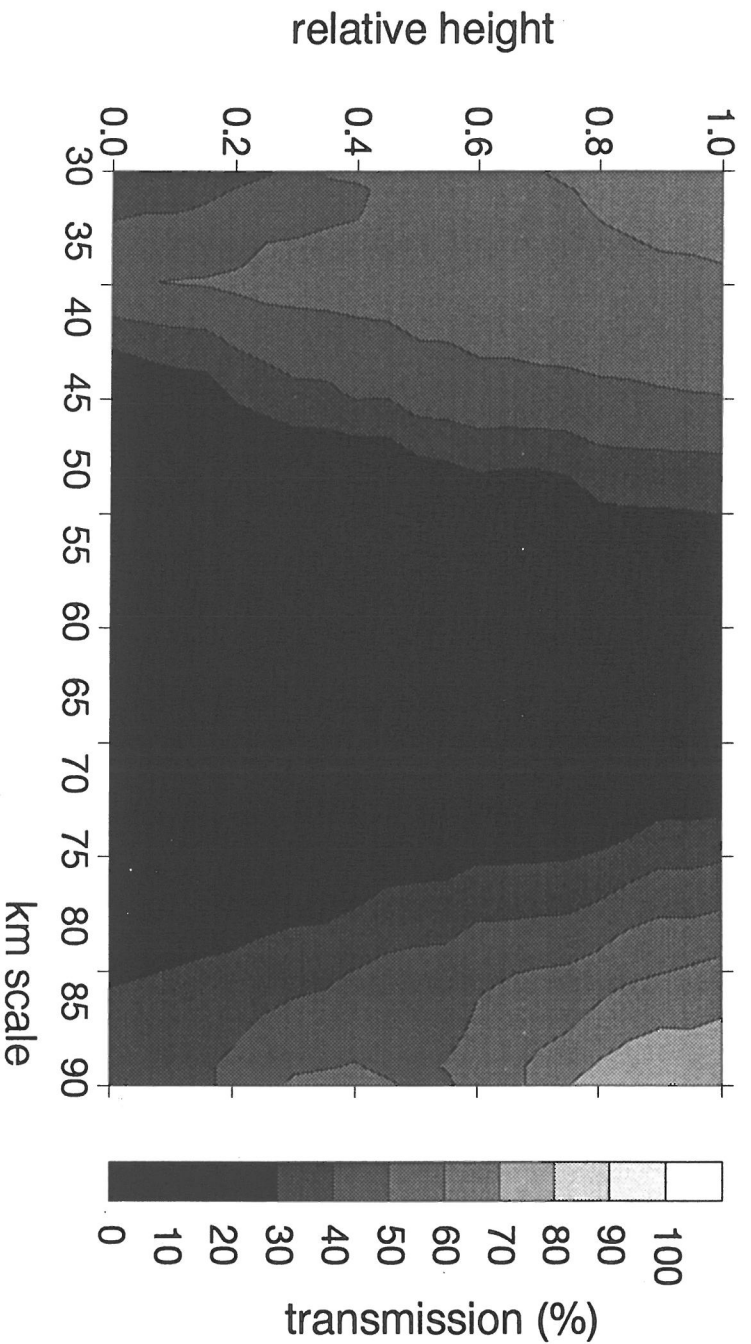
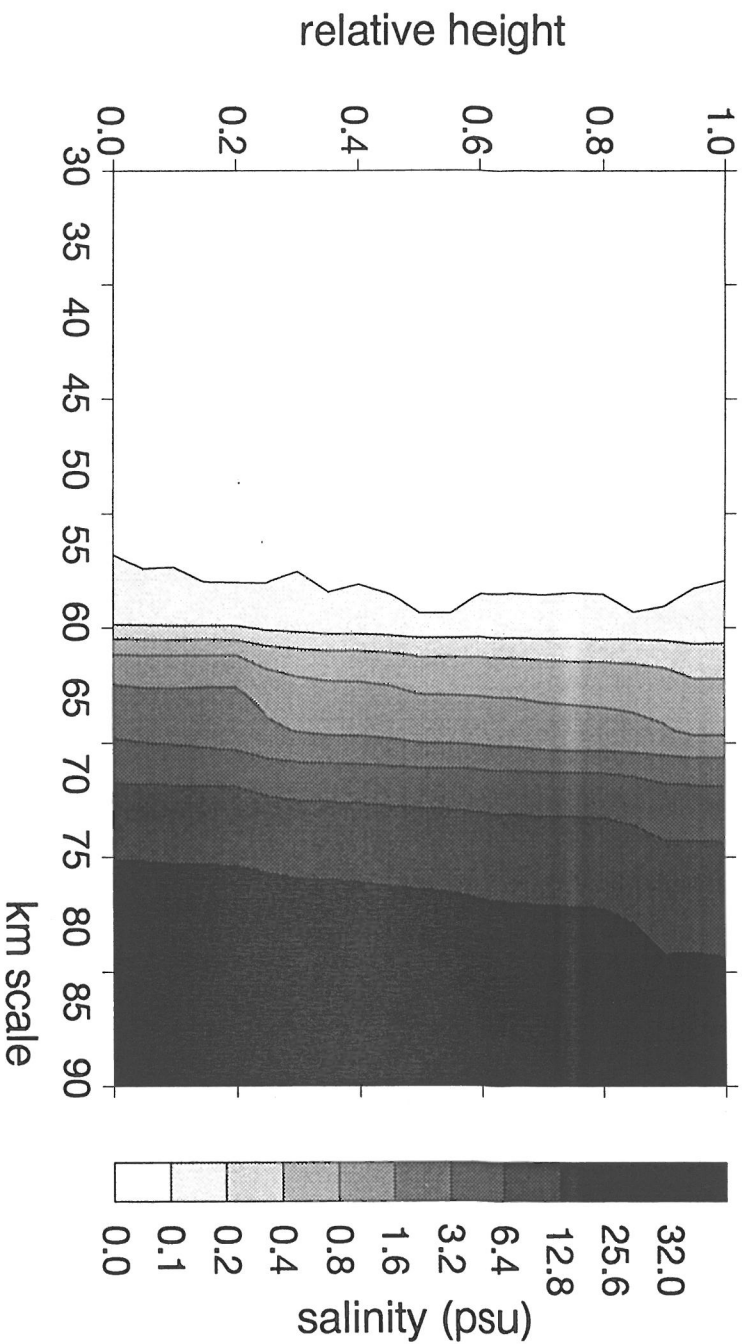


Fig. 7. (a) salinity and (b) light transmission profiles in the first transect, Gironde 1994. The horizontal scale is the longitudinal estuarine axis, the vertical scale is relative height above the bottom (1=surface, 0=bottom).

Schelde 1993 transect 1

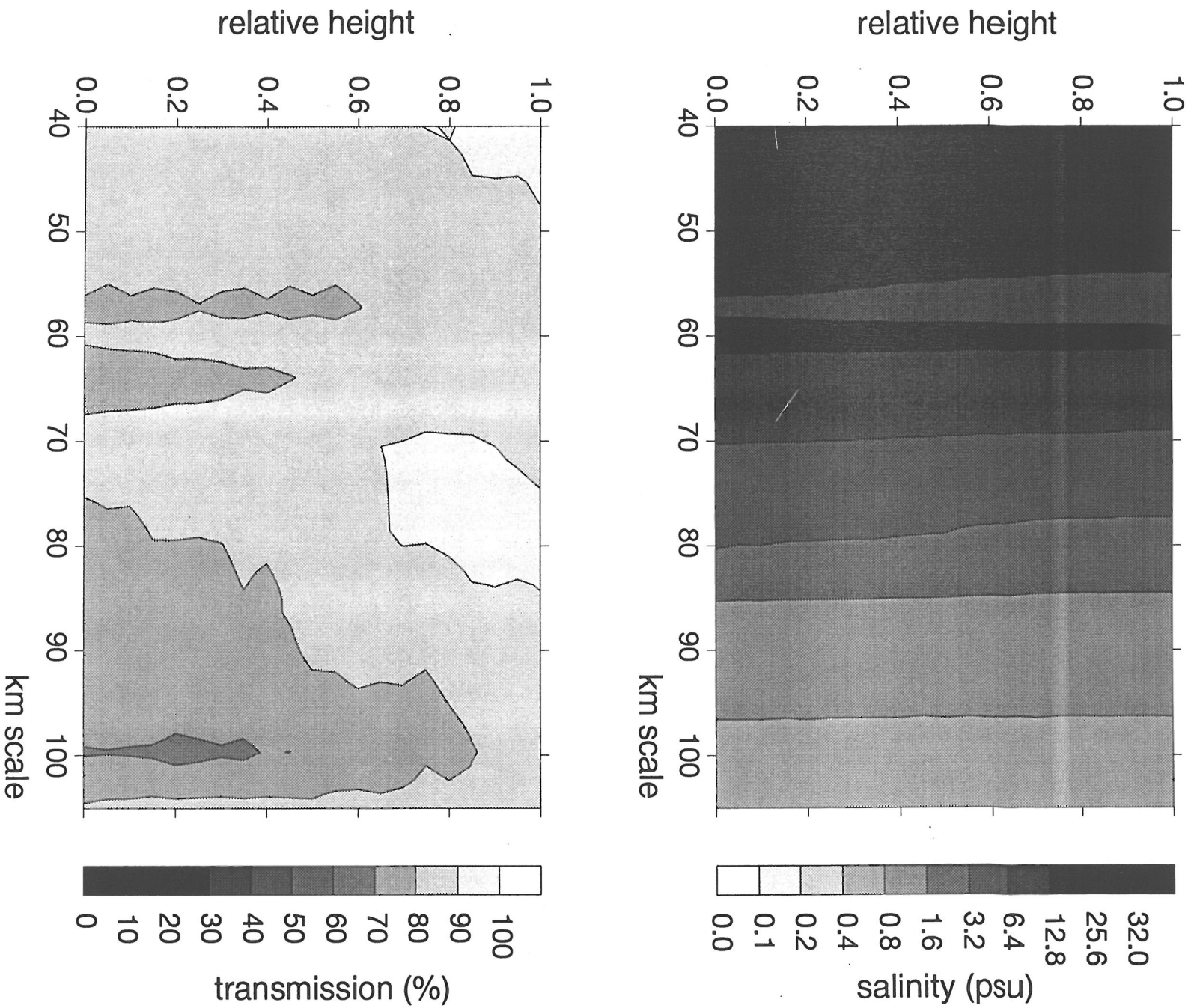


Fig. 8. (a) salinity and (b) light transmission profiles in the first transect, Schelde 1993. The horizontal scale is the longitudinal estuarine axis, the vertical scale is relative height above the bottom (1=surface, 0=bottom).

Schelde 1993 transect 2

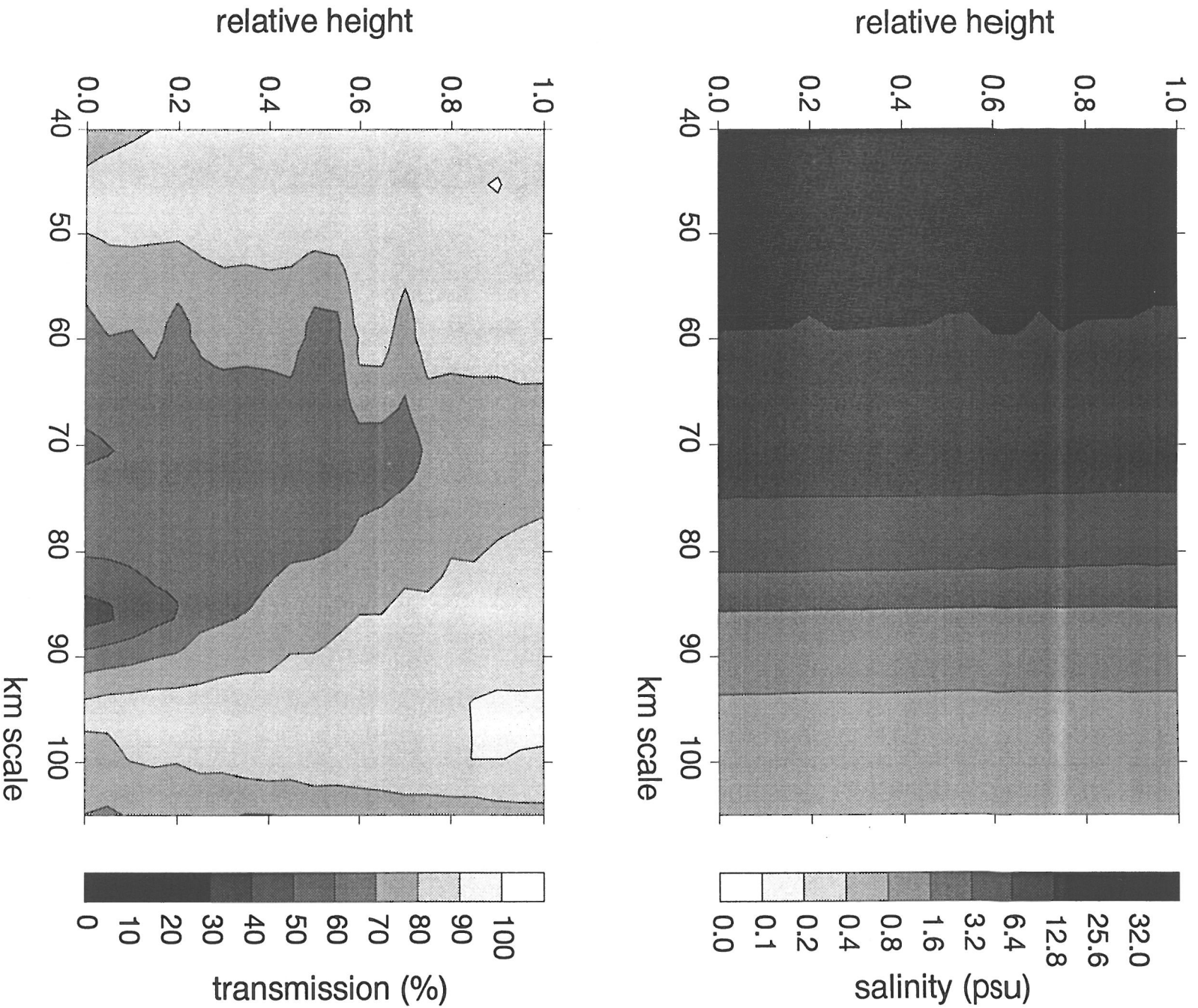


Fig. 9. (a) salinity and (b) light transmission profiles in the second transect, Schelde 1993. The horizontal scale is the longitudinal estuarine axis, the vertical scale is relative height above the bottom (1=surface, 0=bottom).

Schelde 1994 transect 1

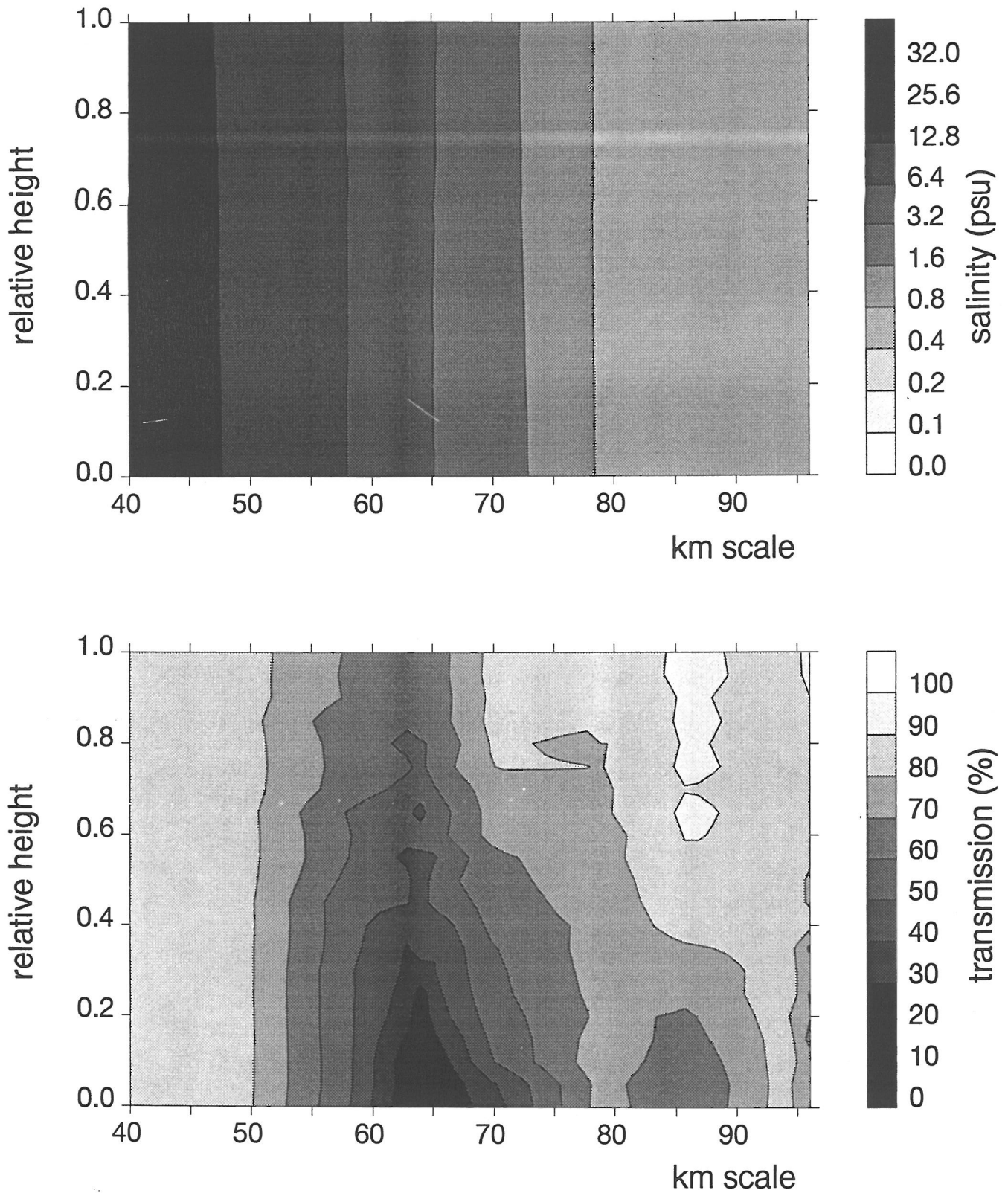


Fig. 10. (a) salinity and (b) light transmission profiles in the first transect, Schelde 1994. The horizontal scale is the longitudinal estuarine axis, the vertical scale is relative height above the bottom (1=surface, 0=bottom).

Schelde 1994 transect 2

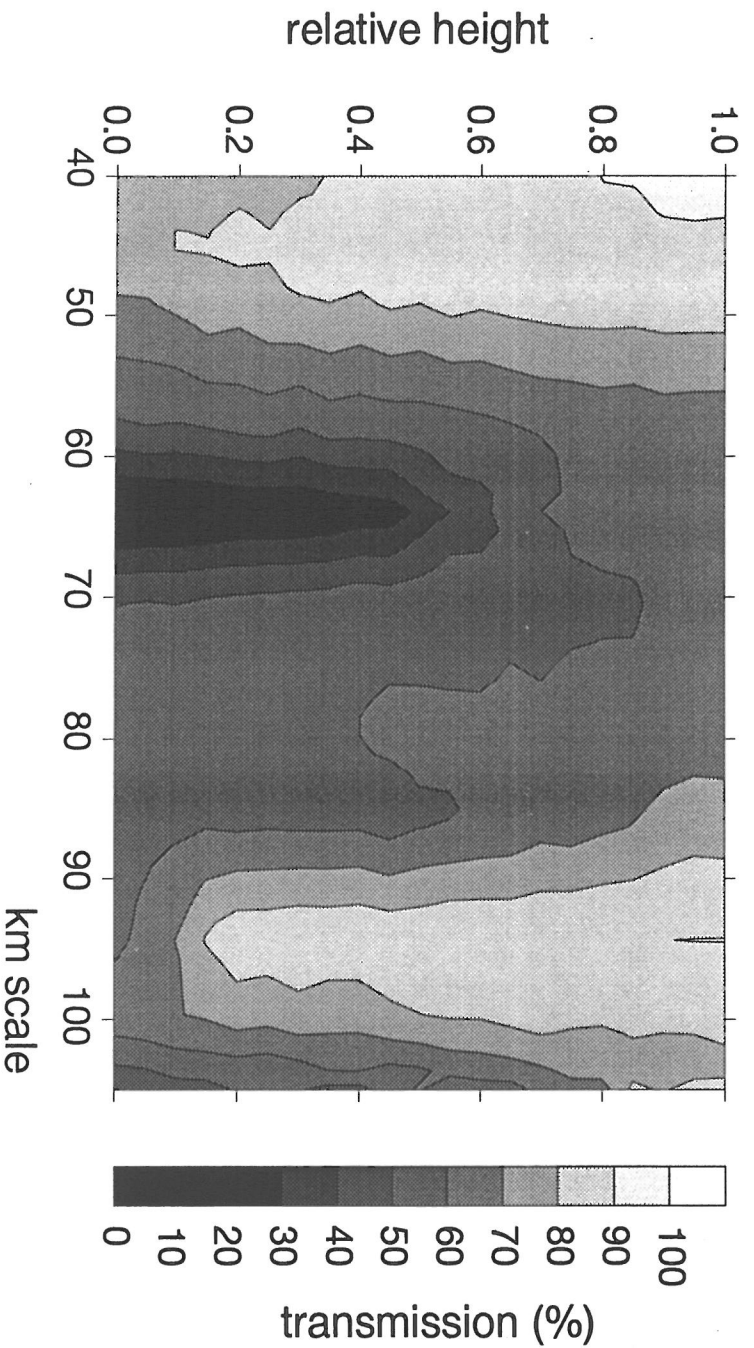
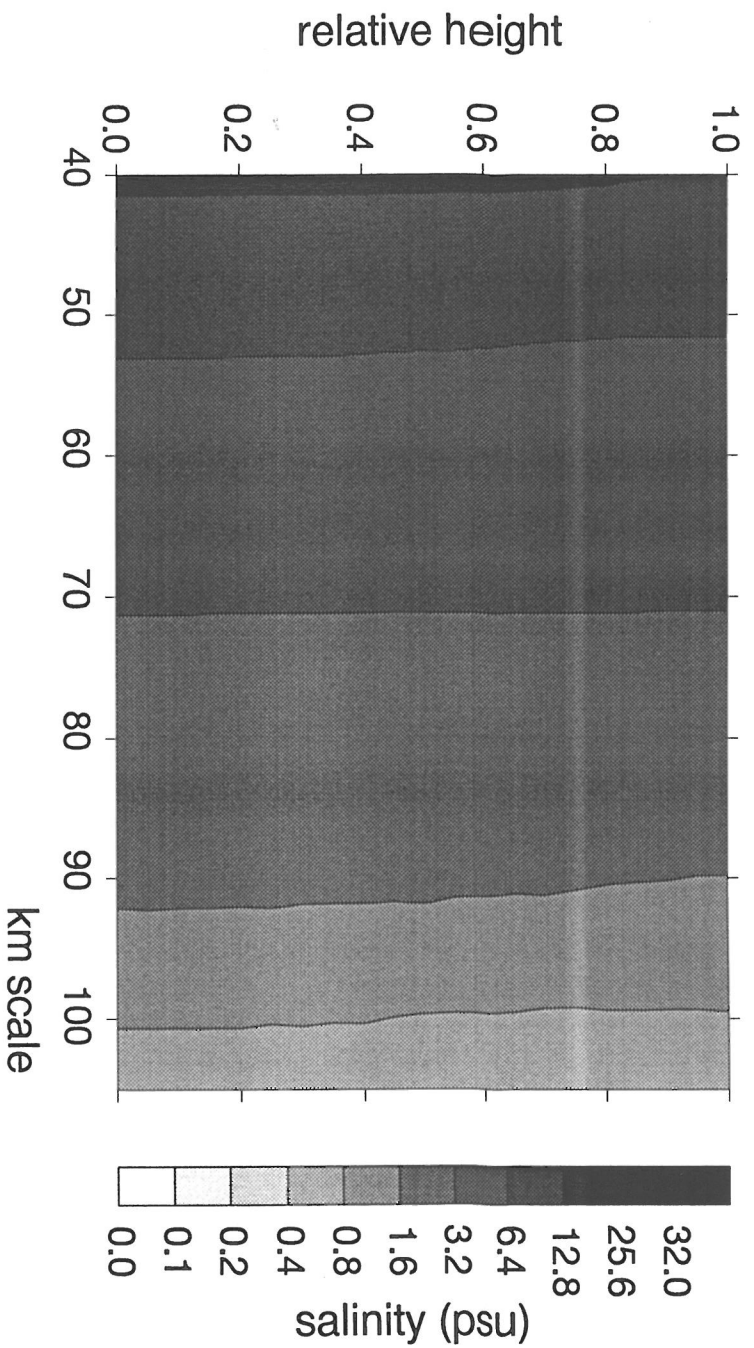


Fig. 11. (a) salinity and (b) light transmission profiles in the second transect, Elbe 1994. The horizontal scale is the longitudinal estuarine axis, the vertical scale is relative height above the bottom (1=surface, 0=bottom).

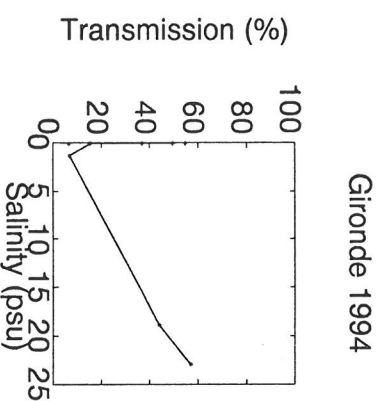
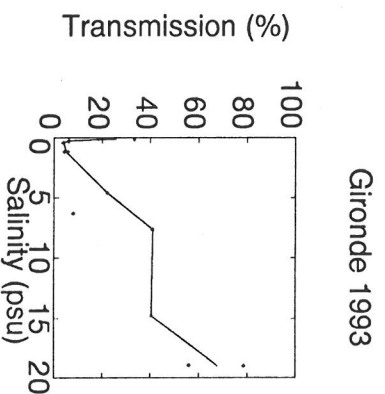
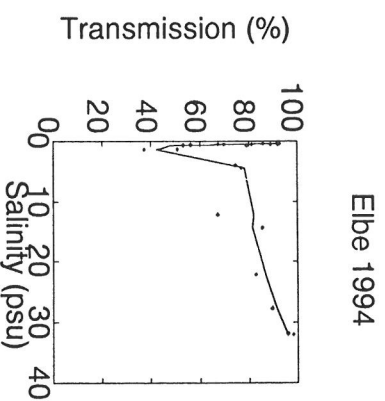
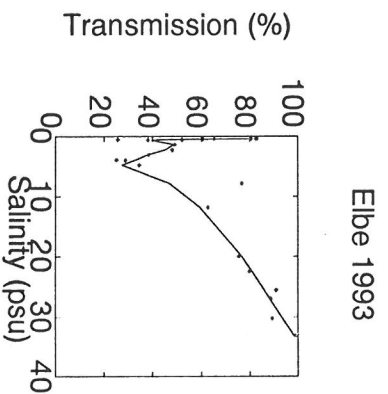
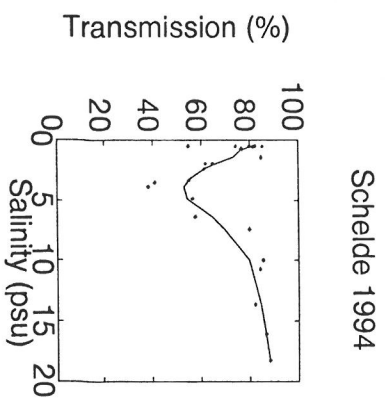
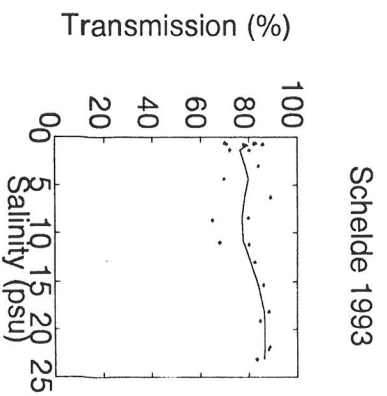


Fig. 12. Relation of column-averaged transmission with column-averaged salinity along the estuarine transects in the three estuaries in the two years of study. Dots represent observations, lines are smoothed values using the non-parametric LOWESS smoother (tension 0.4) (Systat, 1994).

3. The dynamics of suspended matter in the MTZ - flocculation processes.

3.a. The *in situ* determination of floc size.

The dynamics of flocs in the MTZ were studied primarily by *in situ* camera systems (see Eisma, this report, for full details). Two different camera systems were deployed: a camera with a 1:1 image, and one with a 1:10 magnification. The volume of water photographed by the latter camera is appr. 100 times smaller than that covered by the 1:1 camera.

Both camera systems have a different detection window for particle sizes. The mean particle diameter determined with both systems differs by approximately one order of magnitude, although both cameras seem to give consistent results. An example is shown in Fig. 13, where measurements of floc numbers in a size class vs. geometric mean diameter of the class by the two camera systems in one body of water were overlaid, after proper rescaling for the volume of water scanned. In the overlap zone between the two detection windows, averages between both readings were calculated. The consistency shown between the two camera systems was found in most samples where both cameras were deployed quasi-simultaneously.

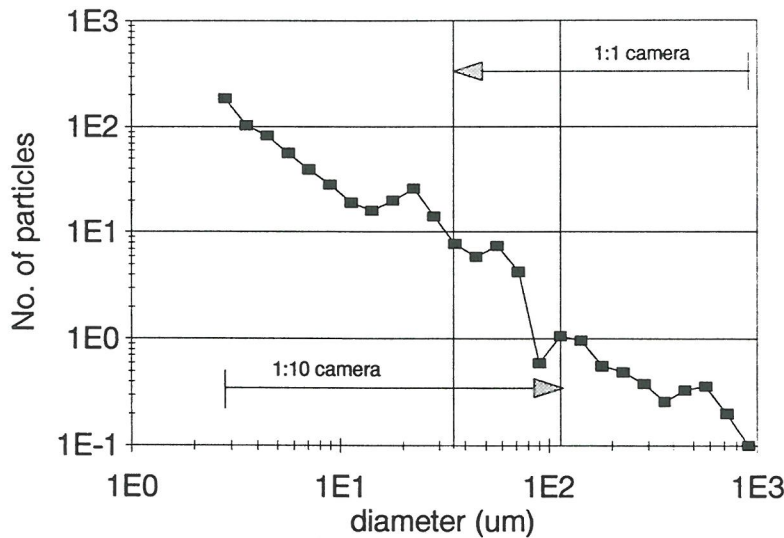


Fig. 13. Comparison of floc size frequencies observed by the two camera systems in the same body of water. Number of particles per size class is plotted vs. geometric mean diameter of the size class. Observed numbers of particles in the 1:1 camera were divided by 100 since this camera scans a 100 times larger volume of water. In the overlap zone, the number of particles was calculated as the average of the rescaled numbers in the two camera readings.

Nevertheless, the (volume-based) mean particle sizes calculated from both cameras have a relatively low correlation coefficient of 0.32 (see Fig.14). This may be caused by scatter in the data, especially in the larger diameter classes which have a large weight in the calculation of the volume-base mean size.

To filter out as much of the variability as possible, we calculated the geometric mean of the volume-based particle size of both cameras as a relative measure of particle size to relate with other measured variables.

In Fig. 15 this geometric mean particle size is plotted against the best predictor we could calculate from the environmental data available in the joint field campaigns. This predictor is expressed as:

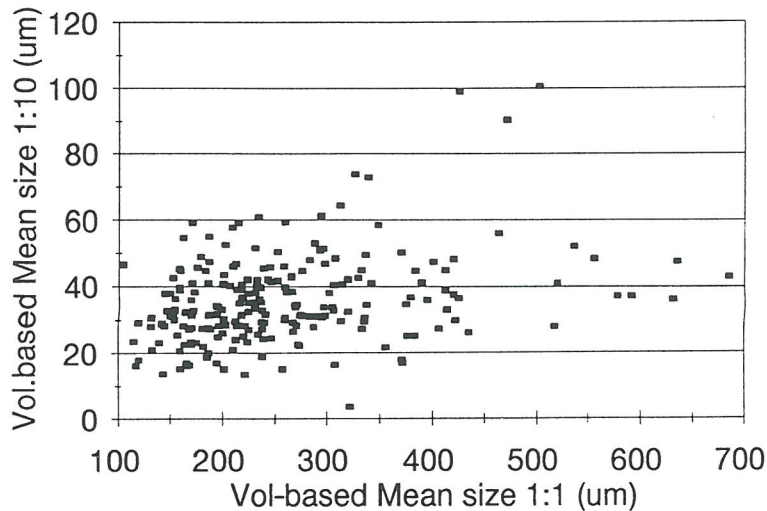


Fig. 14. Relation between the volume-based mean floc size determined by two camera systems in the same body of water. All available data where both camera systems have been used are shown.

$$\log_{10} (\text{Particle size}) = 1.714 + 0.105 * \log_{10} (\text{SPM}) + 0.145 * \log_{10} (\text{POC}) - 0.103 * \log_{10} (\text{SAL}) \quad (\text{eq.1})$$

where SPM = suspended particulate matter concentration (mg.l^{-1})
 POC = particulate organic carbon concentration (mg C.l^{-1})
 SAL = salinity of the water (psu)

This regression had an r^2 of 0.44 ($n=97$) and was highly significant. In view of the rather low correlation between particle sized determined by the two camera systems, its value may actually indicate that most of the non-random variation in the particle size is effectively explained by the three environmental variables.

Among the single environmental factors, POC explains most of the variation in particle sizes. The (log-log) regression of particle size on POC has an r^2 of 0.31. This value is 0.21 for SAL, and 0.15 for SPM.

The result of this regression analysis using the average of the 1:1 and 1:10 camera systems is qualitatively in accordance with regressions of the particle sizes obtained by the 1:1 camera or the 1:10 camera systems on environmental variables separately. We consistently find that POC is the single most important variable in the environment explaining the size of the flocs as observed in the field.

Two main factors are thought to be important for the formation of a floc upon collision between two particles (van Leussen, 1994): the organic coating of the particles and the salinity of the surrounding water influencing the double layer dynamics. The regression equation qualitatively indicates the importance of this coating with the positive exponents for POC and SPM. The influence of salinity is more complex. In the data set particle size decreases with increasing salinity, contrary to what is expected from theory. However, a closer inspection of the data reveals that the influence of salinity is non-linear. Fig. 16 shows the residuals of particle size on POC and SPM (i.e. the difference between observations and the part of the prediction equation containing POC and SPM) as a function of salinity. It can clearly be seen that particle sizes are larger than expected at salinities up to 1 psu, but decrease again at higher salinities. Salinity change (from freshwater to slightly brackish) has a more profound effect than salinity *per se*, possibly because a new equilibrium between organic coating and salinity establishes at higher salinities than appr. 1 psu. It should be noted that, although most observations in this salinity range come from the Schelde estuary, the Elbe observations are fully in line with the Schelde data. Moreover, this zone of low salinities corresponds very well with the observed zones of increased turbulence, as observed in the hydrographic descriptions of the estuarine maximum turbidity zones.

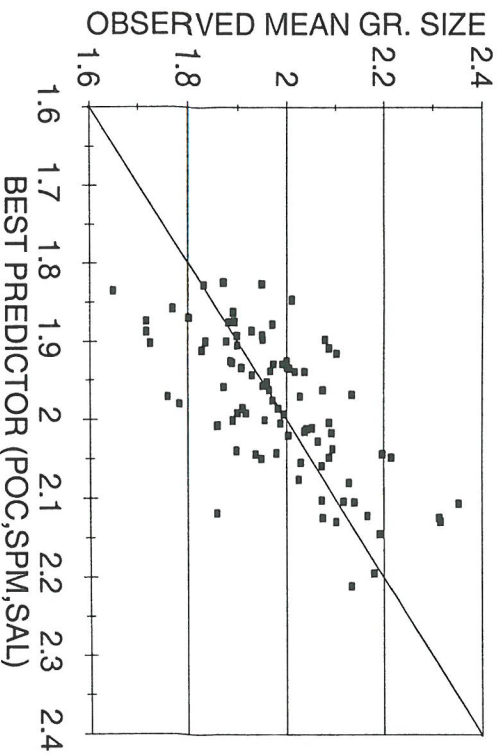


Fig. 15. Relation between predicted and observed mean particle size. Mean particle sizes here are the log-transformed geometric means of both camera systems used. The linear predictor used is explained in the text.

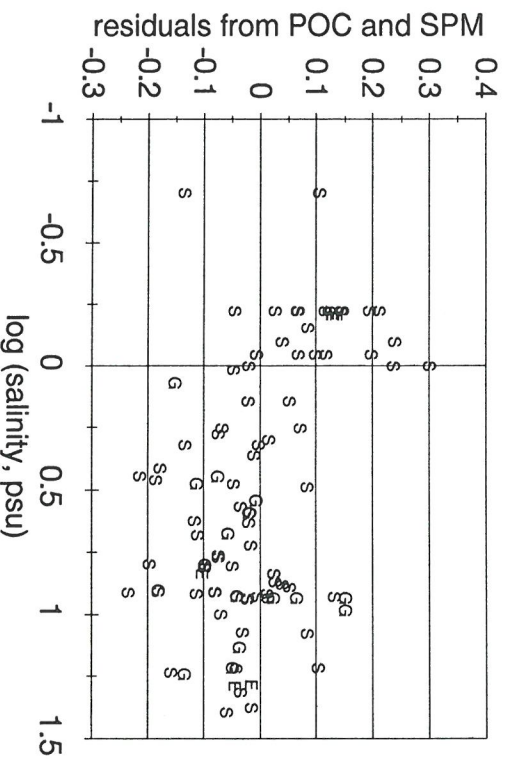


Fig. 16. Dependence of flocculation size on salinity. The ordinate gives the residuals of geometric mean flocculation size from the linear predictor terms for POC and SPM only. The abscissa is (log-transformed) salinity. Highest residuals are found in the 0.1-1 psu salinity range. Letters indicate the estuary sampled.

3.b. Sinking speed of flocs - *in situ* determination.

Eisma (this report) has performed a number of measurements on the sinking speed as a function of flocculation size in the field. We refer to this report for full details. Although considerable scatter is present, the sinking speed of the flocs can best be represented as a function of the minimal diameter of the flocs. The GM regression equation ($r^2=0.23$, $n=50$) describing this relationship is:

$$\log_{10}(\text{sinking speed}) = -2.56 + 1.39 * \log_{10}(\text{smallest diameter}) \quad (\text{eq.2})$$

where sinking speed is given in mm/s and diameter in μm .

The slope of this regression is smaller than 2, the value of Stokes' law that would be applicable to solid spherical particles. This latter value was found by van Leussen (1994) in the Ems Estuary and attributed to the mostly biological nature of the flocculation material. For pure mud

flocs in the laboratory, the exponent is usually in the range of 0.4-1.0 (Gibbs 1985; Hawley, 1982; Kajihara, 1971). The present observations are intermediate between the two extremes.

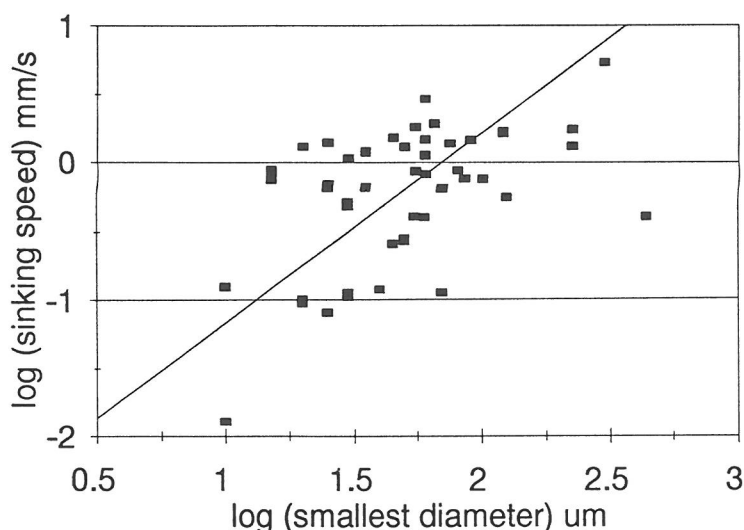


Fig. 17. Relation between observed sinking speed of flocs with smallest diameter of the floc. The regression line is a Geometric Mean regression.

The predicted difference in sinking speed of particles is two orders of magnitude over the size range observed. Combined with the predicted influence of POC on particle size, one can conclude, at least qualitatively, that the organic matter in estuaries is partly responsible for the dynamics of the suspended material. The importance of this factor can be estimated from the exponents of the regressions. Mean particle size variation attributable to POC and SPM was a factor two in our data base, leading to a predicted variation in sinking speeds of slightly over a factor two.

Due to technical difficulties (see: Eisma, this report) the number of determinations of particle settling velocities was too small to re-appraise the relationship between settling velocity and particle concentration in the water. This relationship is important for the hydrodynamical and sediment transport modelling (see: Cancino & Neves, this report). Literature data for the coefficients of the relationship had to be used for the modelling. However, the form of the relationship between settling velocity and suspended matter concentration as used in the modelling (based on Dyer, 1986) is quite similar to the one predicted on the basis of the regression equations presented here.

3.c. Modelling suspended sediment concentration, deposition and erosion.

3-D hydrodynamical and transport models have been developed for the three estuaries (Pfeiffer, this report, Cancino & Neves, this report). Numerical experiments, mainly with the Schelde model, point to several important conclusions.

Local geographical information on sediment composition is important for a correct prediction (at short term) of the suspended sediment dynamics in the water column. The availability of erodable sediment and the critical erosion velocity parameters are dependent on the composition of the sediment. It was shown for the Schelde that correct predictions of the along-estuary gradients in suspended matter concentrations were not possible without allowing for variable coefficients (based on observed sediment composition) along the estuarine gradient. Although obviously the composition of the sediments itself is a function of hydrodynamic factors, modelling at a much longer timescale would be needed to predict it, and thus make the sediment transport modelling self-contained. Models developed within the project make

predictions essentially at the time scale of a tidal cycle; this can only be successfully performed with the inclusion of field data on sediment composition.

The three-dimensional topography of the estuary determines essential features such as vertical mixing, salt stratification, upward bottom flows of suspended sediments etc..., leading to the observed turbidity in the MTZ. This is shown very clearly by the lateral transect in Hansweert (Schelde) taken from the numerical simulations. Vertical gradients result from the specific structure of the northern and southern flow channels. (Fig. 18). In the Gironde, essentially the same model with similar parameters produced much more vertical stratification and a considerably higher turbidity in the MTZ.

The transport models were able to produce hindcasts of the suspended matter concentration and salinity profiles well in accordance with observations during the field work. As such, they provide excellent tools to investigate further the relative importance of mechanisms of suspended sediment dynamics described by the field studies. Inclusion of these mechanisms into the models, however, was not possible due to time limitations of the project.

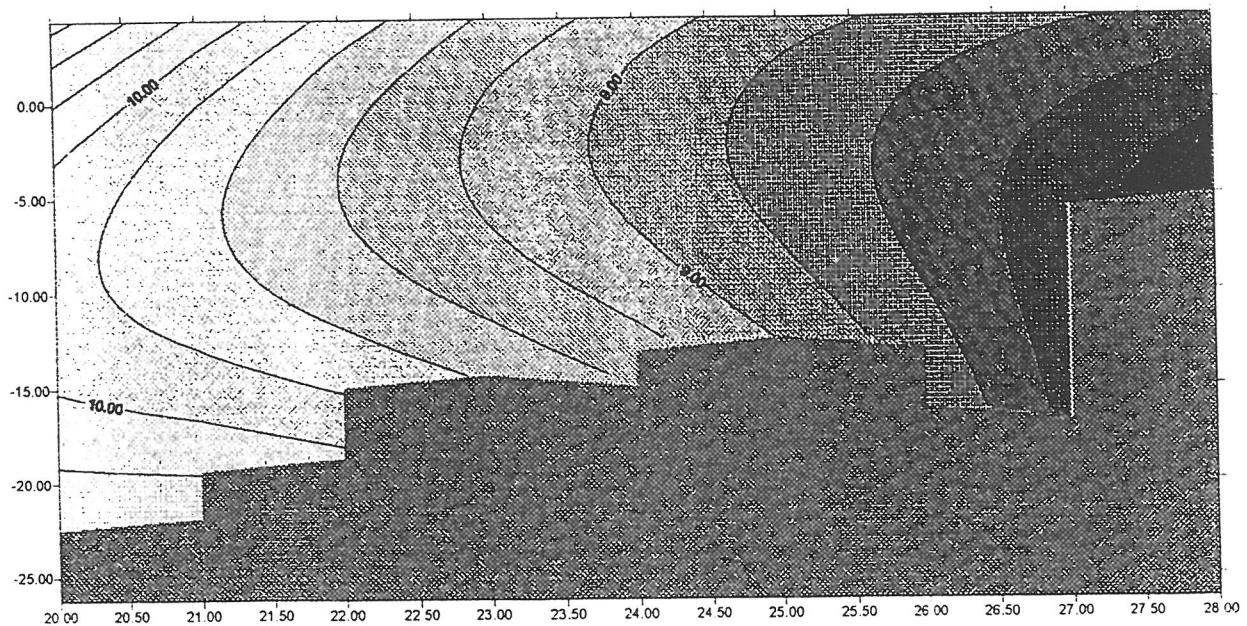


Fig. 18. Model results showing vertical profile of salinity (psu) during low slack water period in a transversal section near Hansweert (simulated for the day 28/04/94). Y-axis gives local depth in meters, X-axis transversal coordinates. (From: Cancino & Neves, this report)

4. The dynamics of organic matter in the MTZ.

During the field programmes, concentrations of POC and DOC have been measured alongside with bacterial numbers, biomass and production, and with physico-chemical variables such as SPM, salinity etc... Besides, chemical characterization of organic material has been done on a limited number of samples from six European estuaries, including Schelde, Elbe and Gironde (Burdloff et al., this report) From these measurements, a number of relationships can be derived.

One hypothesis that was tested is the close association (by adsorption) between inorganic suspended material and organic material in the water column. Adsorption onto the surface of inorganic particles has been shown to be the major factor determining the degradability of organic material in marine sediments (ref.). Since the concentration of inorganic material in the MTZ is much higher than in marine waters, one could hypothesize that adsorption onto the inorganic particles determines the degradation rate and general biological availability of the organic material also in the MTZ of estuaries. This hypothesis provides two testable predictions: the ratio POC/DOC is dependent on the concentration of suspended inorganic material, and the degradation rate constants of organic material in the water column of the MTZ is of the same order of magnitude as that in marine sediments (i.e. much lower than typical marine water column values).

A model representing the adsorption process (assuming equilibrium) is as follows:

$$\frac{\partial POC}{\partial t} = k_1 * SPM * DOC - k_2 * POC = 0 \quad (\text{eq.3})$$

which can be rewritten as (writing $TOC=POC+DOC$ and $K = \frac{k_2}{k_1}$):

$$\frac{POC}{TOC} = \frac{SPM}{SPM + K} \quad (\text{eq.4})$$

This relation was fitted to all data available from the three estuaries in the database. The relationship is shown in Fig. 19. Considering that these data come from three different estuaries in two different years, the fit is good. $K=89.972$, r^2 (nonlinear least squares fit) = 0.524. The estuaries do not separate themselves on the graph. This is remarkable, since in the Gironde both DOC concentrations and the ratio POC/SPM are considerably lower than in the other estuaries.

The reasonable fit of the data to eq.4 is, in itself, no good reason to accept the validity of the model (eq. 3). Several other assumptions could lead to expressions similar to eq.4. E.g. if the concentration of DOC and the ratio POC/SPM were constant everywhere, exactly the same solution would be found. However, the data clearly show variability in DOC and POC/SPM, and moreover the two are correlated (which would not be the case if they were equal to a constant + a random noise term). Similarly, if both DOC and POC/SPM were linearly related to a common factor, expressions like eq.4 can be expected. Salinity is an obvious choice for a common factor. Within each of the estuaries, DOC-concentrations decrease linearly with increasing salinity. For POC/SPM, the linear decrease is less obvious but still suggested by the data. By taking a different upstream concentration for each estuary (especially for the Gironde, where concentrations of both variables are much lower), a good explanation of the ratio POC/TOC by using salinity as an explaining variable can be obtained. However, the problem is then transferred to an explanation of the upstream concentrations, and in particular to an explanation of the apparent correlation between DOC and POC/SPM in the upstream conditions of the different estuaries. This correlation is most probably generally valid. Meybeck (1982) shows that over more than three orders of magnitude variation in SPM in the world's rivers, the ratio POC/SPM varies over less than two orders of magnitude, and the ratio DOC/TOC is generally between 0.1 and 0.9. This pattern is only explainable if DOC co-varies with the ratio POC/SPM. Decisive evidence on this problem, however, should come

from kinetic studies on the relation between organic and suspended matter in estuaries. This is an area for experimental research.

A second prediction of the adsorption hypothesis concerns a relatively low bacterial degradation rate of the organic material adsorbed onto inorganic particles. Degradation rate of the organic matter has not been determined directly in the present research project. However, from measurements of bacterial production by thymidine uptake (Goosen et al. this report) one can estimate roughly the relative rate of breakdown of the dissolved and particulate organic matter. We regressed bacterial production rate on POC and DOC in the following multiple regression model:

$$\text{BAPR} = -.66 + .35 * \text{DOC} + 0.14 * \text{POC}$$

Bacterial production rate ($\mu\text{g C l}^{-1} \text{h}^{-1}$) was temperature-corrected using a Q_{10} of 2.5. Due to the error structure of bacterial production (multiplicative error), fitting was performed after log-transforming both sides of the equation. r^2 of this non-linear estimation was 0.77. Fig. 20 shows the correspondence between predicted and observed temperature-corrected bacterial production in the three estuaries.

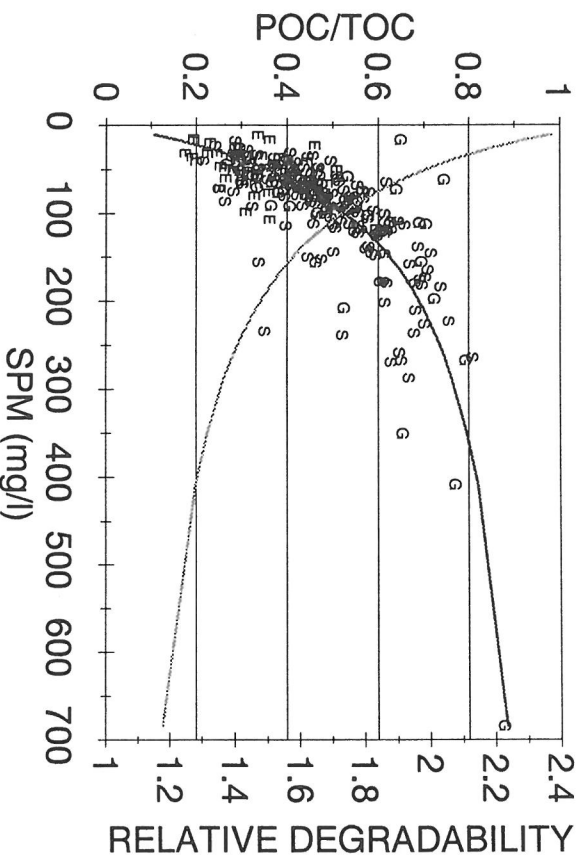


Fig. 19. Fitting of the Langmuir relation between the ratio POC/TOC and the suspended matter concentration in all field samples from three estuaries and two years. Samples from the estuaries Schelde, Elbe and Gironde are indicated by S, E and G respectively. Relative degradability is based on bacterial production rates. A value of 1 corresponds to the degradation rate of POC. Degradability of the organic material, relative to the degradation rate for POC, increases with decreasing particulate fraction.

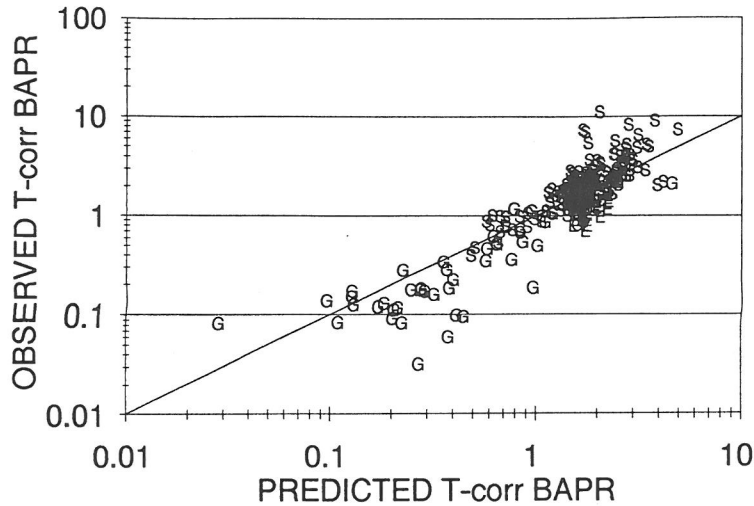


Fig. 20. Comparison between observed (temperature-corrected) bacterial production rate ($\mu\text{g C l}^{-1} \text{h}^{-1}$) and predictions based on a linear function of POC and DOC concentrations. Data are labeled by the first letter of the estuary sampled. For comparison the 1:1 line is also given.

With an r^2 of 0.77 most of the variation in bacterial production rates is described as a simple function of substrates available. It was not possible to relate any of the remaining variance to a measured environmental variable, such as SPM or salinity. Strikingly, the largest deviation between observation and model occurred in a few samples from the Hoboken-Rupelmonde region in the Schelde, both in 1993 and in 1994. This is the region of maximal nitrification activity, and maybe the deviation bears some relationship to that. However, it was not possible with the data obtained to go deeper into this problem. (Fig. 21)

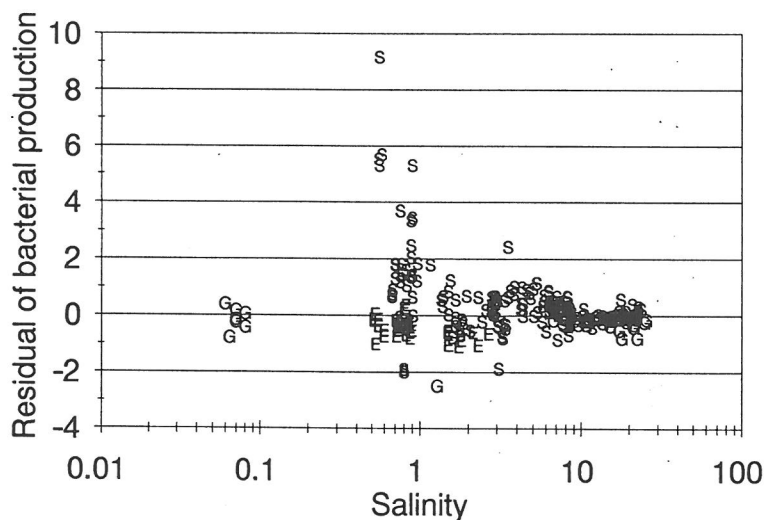


Fig. 21. Residuals of bacterial production rate ($\mu\text{g C l}^{-1} \text{h}^{-1}$) from the regression on POC and DOC, plotted versus salinity. Data are labeled by the first letter of the estuary sampled. Large positive residuals are found in the low-salinity zone of the Schelde estuary only. Based on data by Goosen et al. (this report).

The plot of residuals vs. estimates indicates a slight curvilinearity in the relationship between bacterial production and substrate. In fact, a slightly better regression could be obtained with a power function regression: $\text{BAPR} = A * \text{DOC}^B * \text{POC}^C$, but the increase in fit was not very

high, and this relationship has the disadvantage of being difficult to interpret in biological terms.

The bacterial production rates are not very high, considering the important amount of organic matter present in most samples. By assuming that organic matter decay rate = 2* bacterial production rate, and recalculating units, we conclude that the first order decay rates of DOC are in the order of 6 yr^{-1} , and for POC in the order of 2.4 yr^{-1} . These rates are low, and comparable to first-order degradation rates of organic matter in sediments. This is further evidence that processes in the MTZ are in several respects more comparable to sediment processes than to typical water column processes. The organic matter present is resistant to bacterial degradation; apart from adsorption onto particulate matter, this is probably also caused by the lack of local primary production as a consequence of light limitation (see Kromkamp et al., this report).

The difference in decay rates of POC and DOC is important for the evaluation of the consequences of accumulation of inorganic material in suspension in the MTZ. While the inorganic material is a factor retaining the organic matter in the MTZ, it is also responsible (through adsorption) for a slow-down of the degradation of this organic matter. The relative degradation rate (taking the rate of POC as 1) is added to the figure showing the influence of SPM on organic matter partitioning between POC and DOC. The dependence of degradability on SPM is most pronounced in the range of SPM between 0 and 100 mg/l.

The results of this analysis do not lend support to the hypothesis that the high amounts of suspended matter provide the bacteria with 'reaction centres', through their attachment on the particulate matter. Enhancement of the degradability at high particulate concentrations is not found, on the contrary. However, this does not preclude that the availability of substrate may be of importance to nitrifying bacteria (that have a clear preference for attachment to particles) or for denitrifying bacteria (that are dependent on anoxic microsites). For bacteria in general, Hernandez et al. (this report) show that the percentage attached to particulate material increases with increasing suspended matter concentrations, with decreasing salinity and with decreasing oxygen concentrations. The cross-correlation between these factors clearly shows that bacteria in the MTZ are much more attached to particulates than elsewhere in the estuary.

Measurements performed to investigate the effects of attachment on processes did not yield conclusive evidence. Bonin et al. (this report) report a weak correlation between measured denitrification activity and suspended matter concentrations in the three estuaries. This correlation holds true in most cases for the location of the peak activity along the estuarine transect only. These authors, however, also show that the highest denitrification activity in depth profiles of Elbe and Gironde is found in the surface waters. Considering the generally observed depth profiles of suspended matter, with distinctly higher concentrations near the bottom, this observation would rather point to a negative correlation between denitrification activity and presence of flocs in the water column. The measurements of denitrifying activity by N_2O production are in general very high. In fact, most are higher than the potential denitrifying enzyme activity measured in the same samples, and the order of magnitude of measured denitrification rates would, in combination with estuarine residence times in the order of tens of days, deplete almost all available NO_3 from the water. Possible interference of nitrification with the N_2O production (used to measure denitrification rate) would need more detailed research.

In general, variation in bacterial density or biovolume was limited (Hernandez et al., this report). Biovolume per cell varied over a range of appr. 2, while densities generally ranged between $2 \cdot 10^6 \text{ ml}^{-1}$ and 10^7 ml^{-1} . This variation is considerably less than the variability in bacterial production rates. Bacterial numbers or biomass are a bad predictor of bacterial activity rates.

5. Quality of organic matter - chemical analysis.

Burdloff et al. (this report) analyzed the quality of organic matter in 6 different estuaries by chemical analysis. (Fig. 22). They measured bulk organic material, and also the more de-

gradable fractions proteins, lipids and carbohydrates (PGL). The main conclusion from their study is that the fraction PGL in the organic matter decreases with increasing suspended matter load. Interestingly, this decrease is by a factor of about 2.5 over a similar range of SPM as used in the studies of bacterial production.

It is unsure how these results can be reconciled with the hypothesis of sorption of the organic matter onto inorganic particles. One possibility is that the chemical extraction methods are less efficient when the organic matter is sorbed onto inorganic particles. Another possibility is that in high turbidity environments of Gironde and Ems the organic material is older and more refractory than in the other estuaries, but that this effect was masked in the regression analysis of bacterial production on POC and DOC.

Quality - 6 European estuaries

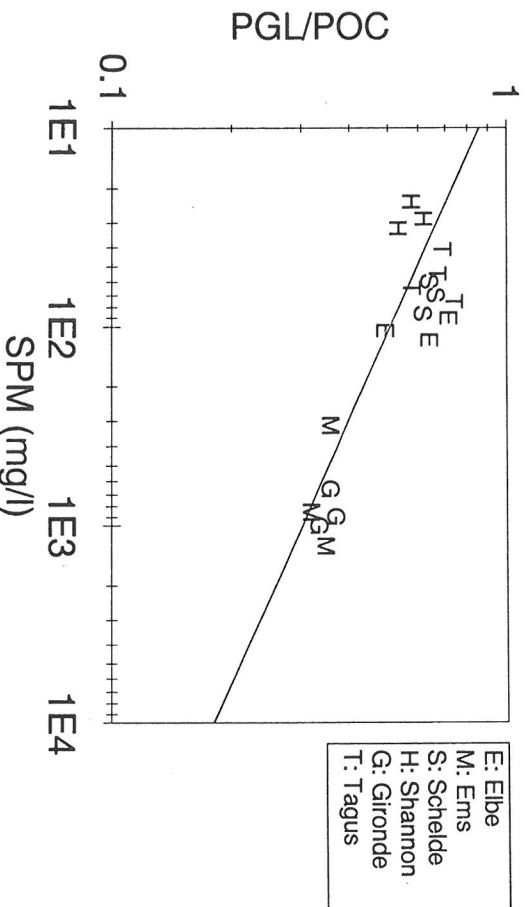


Fig. 22. Quality of the suspended particulate organic material, as expressed by the ratio PGL/POC, versus total suspended matter concentration. PGL stands for the sum of extractable proteins, carbohydrates and lipids. From: Burdloff et al., this report.

6. Phytoplankton and primary production

Phytoplankton in the Gironde was rare, and different from the other estuaries. Phytoplankton assemblages are not very different between the polyhaline zones of Elbe and Schelde. In the limnetic parts, some important differences were noted between the two estuaries. These are probably related to residence time, as there are indications that in the Schelde an autochthonous population for the oligohaline zone developed (see...for details). The shift in species composition between freshwater and estuarine assemblages occurred more upstream of the MTZ in the Elbe than in the Schelde. This is probably related to more intensive grazing (almost absent in the Schelde due to oxygen stress).

In the Gironde phytoplankton biomass is so low that it must be assumed that zooplankton can live of other food sources. These detrital (organic matter) food sources are tightly related to suspended matter in the Gironde, and thus optimal locations should probably coincide with the maximum turbidity zone.

By and large, light limitation is the most important factor determining primary production rate in the three estuaries (see Kronkamp et al., this report). Calculated depth-integrated primary

production for a standard day (i.e. calculated with the observed P-I relationship, assuming the same illumination at the water surface and the same daylength, and corrected for temperature differences with a Q_{10} of 2.5) is strongly dependent on light extinction in the water column, as expressed by the dependence of production per unit biomass on the euphotic depth Z_{eu} (Fig. 23).

The relationship between depth-integrated primary production and euphotic depth is not the same for the three estuaries. There is a significant difference in slope between Gironde on the one hand, and Schelde and Elbe on the other hand. This difference in slope is surprising at first sight: the phytoplankton of the Gironde is the worst adapted to low light regimes, while this estuary has the lowest light intensities in the water column. Most probably the lack of a genuine estuarine phytoplankton assemblage in the Gironde may explain this pattern. Primary production in the maximum turbidity zone of the Gironde is very low; only at the most seaward stations there is a substantial production. The low production in the maximum turbidity zone is performed by marine phytoplankton species that are badly adapted to the turbid estuarine environment, but not replaced by estuarine species because net productivity is negative even for these species. It should be kept in mind that these measurements are taken in 1994, when due to high river runoff the maximum turbidity zone was near to the estuarine mouth.

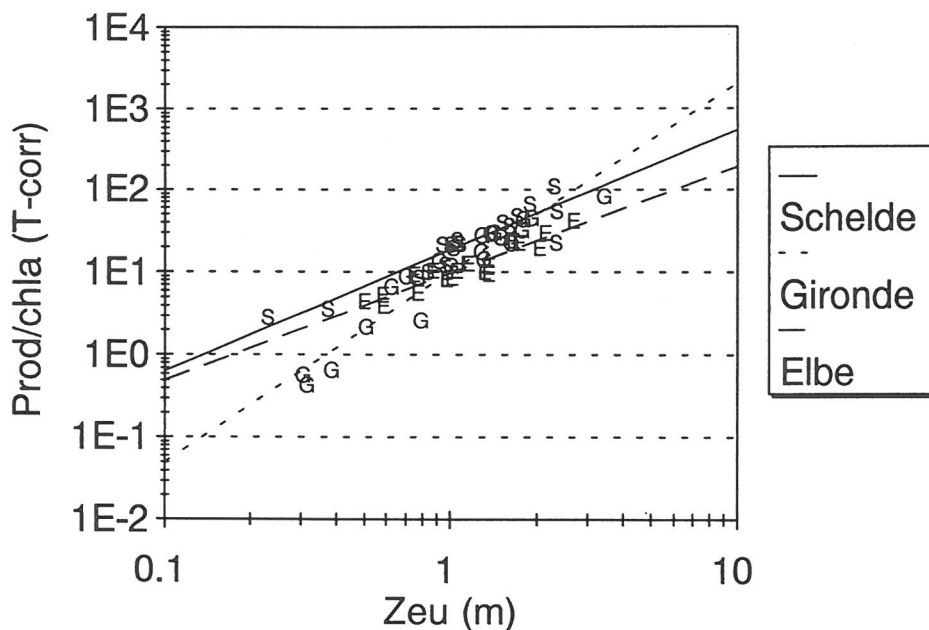


Fig. 23. Depth-integrated, daily-integrated primary production per unit of chlorophyll-a for a standard day along transects in the three estuaries ($\text{mgC m}^{-2} \text{d}^{-1} \cdot (\text{mg Chla m}^{-3})^{-1}$), plotted versus euphotic depth. Each normalized production estimation is based on measured light extinction coefficient at the sampling point, and on measured P-I curves at that point. Slopes for Schelde and Elbe are not significantly different, slope for the Gironde is significantly higher. Data from Kromkamp et al. (this report)

In general, production per unit of phytoplankton biomass is very low in these samples. Assuming as an approximation an average depth of 10 m at these stations, a carbon-to-chlorophyll ratio of 30 for the phytoplankton and the standard light and daylength values used in these calculations, gross primary production is on average only 7.5 % of phytoplankton standing stock per day. Taking into account the respiration of the phytoplankton, net primary production was most probably negative in most stations studied.

The limited role of phytoplankton primary production for the organic matter dynamics in the MTZ is further emphasized by calculating the ratio of gross primary production on total organic carbon. The average ratio for the samples taken is 0.39 % per day. Allowing for phytoplankton respiration, this ratio approaches zero or negative values in most of the stations.

7. Higher trophic levels: occurrence

An interesting observation is made by Gasparini et al. (this report), on the shift of developmental stages of *Eurytemora* in Gironde and Elbe (Fig. 24), but not in the Schelde. Two alternative hypotheses are brought forward to explain this spatial distribution: (1) nauplii drift downstream and copepodites move upstream by active swimming, where swimming speed is dependent on body size or (2) specific gravity of animals increases as they grow older, and therefore nauplii would preferentially occur in surface waters with a net downstream current, whereas copepodites would occur in the bottom waters where the residual current is upstream.

Although the available data are not sufficient to reach a conclusion on the mechanism, several factors are in favour of the first hypothesis: measured swimming speeds of *Eurytemora* are sufficient for the displacement made; the spatial distribution of *Eurytemora* with respect to suspended matter in the estuary is different for the three estuaries (coinciding with MTZ in the Gironde, upstream of MTZ in the Elbe, downstream of MTZ in the Schelde); in the Schelde the spatial distribution of the species suggests that it is actively avoiding the low oxygen zone, even if this has the highest potential food concentration; no clear gradients in the vertical distribution of the species have been found in long time series in the Gironde. The investigation of this problem with the aid of the numerical transport models developed within this project is an interesting topic for future research, since the retention of autochthonous estuarine populations within or around the MTZ is fundamental to the understanding of the ecological processes in this area.

The occurrence of hyperbenthos along the transects in the three estuaries (Fockedeey & Mees, this report) bears little correlation with the environmental factors measured, except for the strong avoidance of low oxygen levels in the Schelde. In the Gironde the hyperbenthos has its peak occurrence in the most upstream station, well ahead of the MTZ. In the Elbe it is slightly upstream of the MTZ, whereas in the Schelde it is downstream of the MTZ. Densities in the Schelde are lower than in the other estuaries, but considering the temporal variability known from this estuary it is unclear whether this difference is significant.

Higher trophic levels: food biology

Several studies have been directed towards the influence of abiotic and biotic factors on the food uptake by zooplankton and hyperbenthos.

Fockedeey & Mees (this report) describe the feeding behaviour of *Neomysis integer* as selective towards zooplankton. Besides zooplankton, the animals have (sometimes large) amounts of non-specified detritus in the guts. Qualitative chemical analysis of the material is currently going on. In future descriptions of the dynamics of hyperbenthic animals in the estuaries, a closer connection with the zooplankton stocks is certainly a point of interest. The problem is important since previous studies have shown that hyperbenthic animals may provide an important link between primary production and mineralization processes in the estuary and fish productivity.

Tackx et al. (this report) performed experiments on selective feeding by *Eurytemora affinis* on phytoplankton. They showed that the copepod has a significant preference for phytoplankton, even in the presence of relatively high concentrations of (partly organic) suspended matter. The species can therefore not be described as a non-selective filter feeder, taking phytoplankton and detrital food in the proportions offered to them. Gut fluorescence measurements in many samples differing in chlorophyll content and suspended matter (Gasparini et al., this report) confirm these observations, but define more clearly the conditions under which selectivity may operate. As shown in Fig. 25, no correlation was found between gut fluorescence and chlorophyll concentration in the water. A clear negative correlation was observed between gut fluorescence and suspended matter concentration. Egg production rates are lower at higher suspended matter concentrations, but the decrease is less pronounced than that of gut fluorescence, showing that the animals com-

pensate for the lack of phytoplankton food by a higher intake of non-fluorescent food particles.

A few simple model calculations, using observed data on POC, SPM and CHLa in the MATURE database (and, thus, taking into account the field correlations between these variables), explore the possible impact of selectivity of the copepods. Assuming that the species feeds non-selectively, uptake of chlorophyll-a would be proportional to the fraction chl-a in the total POC. If total uptake rate of POC is described with a Monod function, gut fluorescence would be given by:

$$GF = a * POC / (K + POC) * chl-a / POC$$

where GF is gut fluorescence recalculated as a dimensionless (gC/gC) ratio, a is a proportionality constant, POC is total particulate organic carbon (mg.l⁻¹) and chl-a is chlorophyll a concentration recalculated to mg C.l⁻¹ with a C/chl-a ratio of 50.

Predicted gut fluorescence under these assumptions is given as a function of SPM and of chlorophyll-a in Fig. 26a,b (where a=0.04, K=4 mg.l⁻¹). A clear relationship with Chl-a is shown, contrary to the observations.

As an alternative, one could assume that the copepods' clearance rate (volume swept clear per individual per unit time) is inversely proportional to chlorophyll-a concentration (animals look for phytoplankton food in larger volumes when this is rare) and inversely proportional to POC concentrations (high concentrations demanding more handling time for the particles). Further, one could assume that the animals take all phytoplankton food from the cleared volume, but only a small proportion of the POC. Gut fluorescence would then be given by:

$$GF = a * chl-a * \frac{1}{K_c + chl-a} * \frac{1}{K_p + nPOC}$$

where K_c (mg C l⁻¹) and K_p (mg C l⁻¹) are saturation constants preventing the clearance rates from becoming infinite, chl-a is the phytoplankton concentration recalculated to mg C l⁻¹, nPOC is the non-phytoplankton POC (mg C l⁻¹), GF is a non-dimensionalised ratio and a (l (mg C)⁻¹) is a proportionality constant.

Figs. 26c,d (where a=0.0275 l (mg C)⁻¹, K_c= 0.005 mg/l and K_p= 1 mg l⁻¹) show that this model cannot be refuted by the data. Both the dependence of gut fluorescence on SPM, and the non-dependence on chlorophyll-a concentration, are reproduced. The constants of the model are chosen such that the order of magnitude of predicted gut fluorescence corresponds to the data in Fig. 25. Moreover, taking into account the gut passage time used by Irigoien et al.(), the clearance rate for phytoplankton was calculated without any other change to the model than recalculation of units. Its value is in the range measured by Tackx et al. (this report). The dependencies of phytoplankton clearance rate on phytoplankton biovolume (shown in Fig. 26e), total particulates volume and ratio phytoplankton/total particulates (not shown here) faithfully reproduce the figures given by Tackx et al. (this report). These features corroborate the simple model proposed here.

This model can be interpreted such that the animals take all phytoplankton food particles from the volume of water cleared per unit of time, and complete their feeding by uptake of a relatively small proportion of the non-phytoplankton POC in this volume. Assuming that the maximal gut content (calculated as a dimensionless ratio) is in the order of 0.02, one can calculate the non-phytoplankton gut content as 0.02-GF. Thus an apparent selectivity can be calculated as the ratio between relative concentration of phytoplankton POC in the gut over relative concentration of phytoplankton carbon in the water. (relative concentration being taken as concentration of phytoplankton divided by total POC, either in the gut or in the water). The apparent selectivity is almost independent of POC, but is a strong negative function of chlorophyll-a concentration. Under this model, we expect the highest apparent selectivity indices when both chlorophyll-a and POC are low, but an almost equally high selectivity at low chlorophyll-a and high POC.

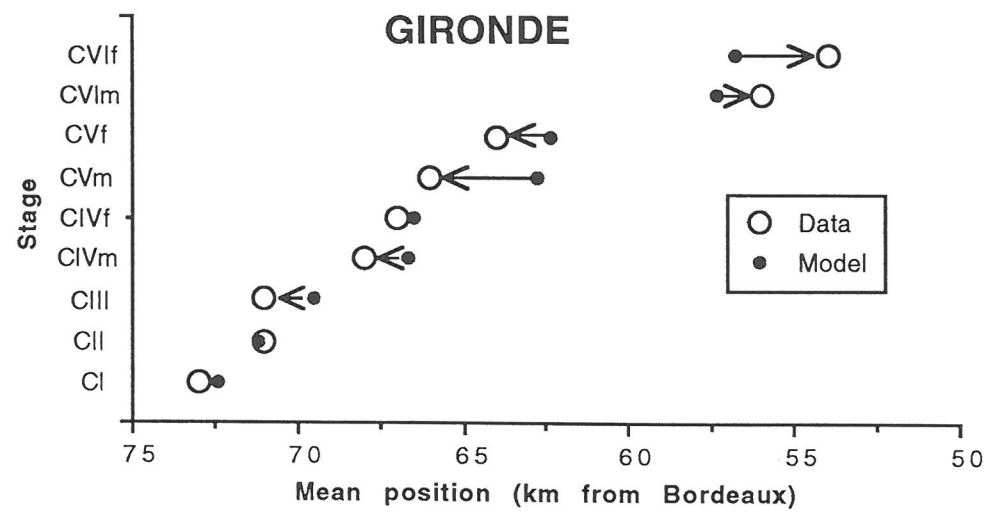
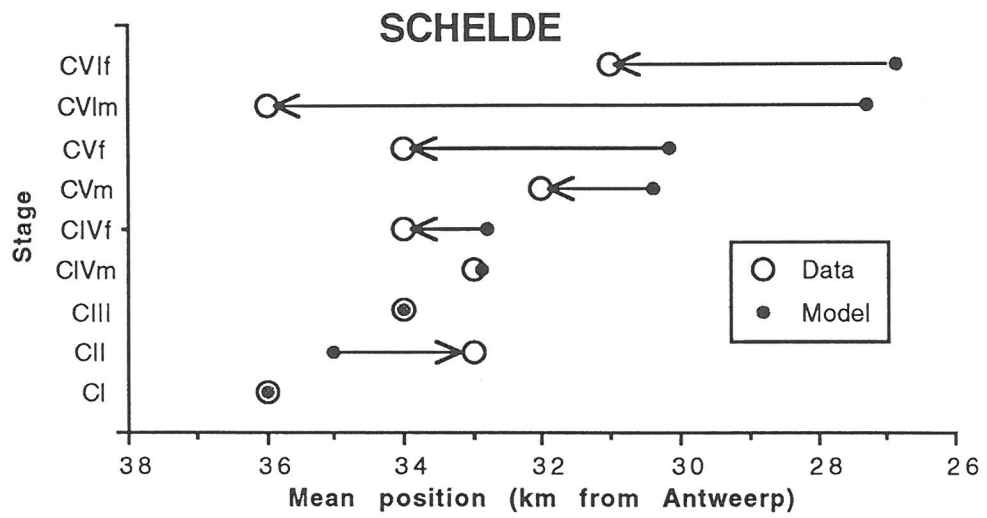
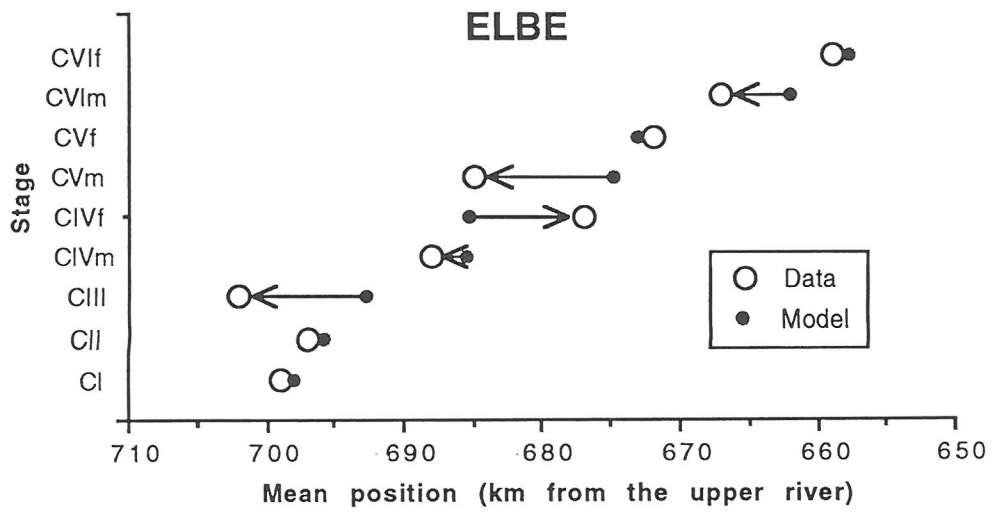


Fig. 24. Distribution of developmental stages of *Eurytemora affinis* along the axis of the estuaries Elbe, Schelde and Gironde. 'Model' values are calculated taking into account size-dependent swimming speeds of the animals. From: Gasparini et al., this report.

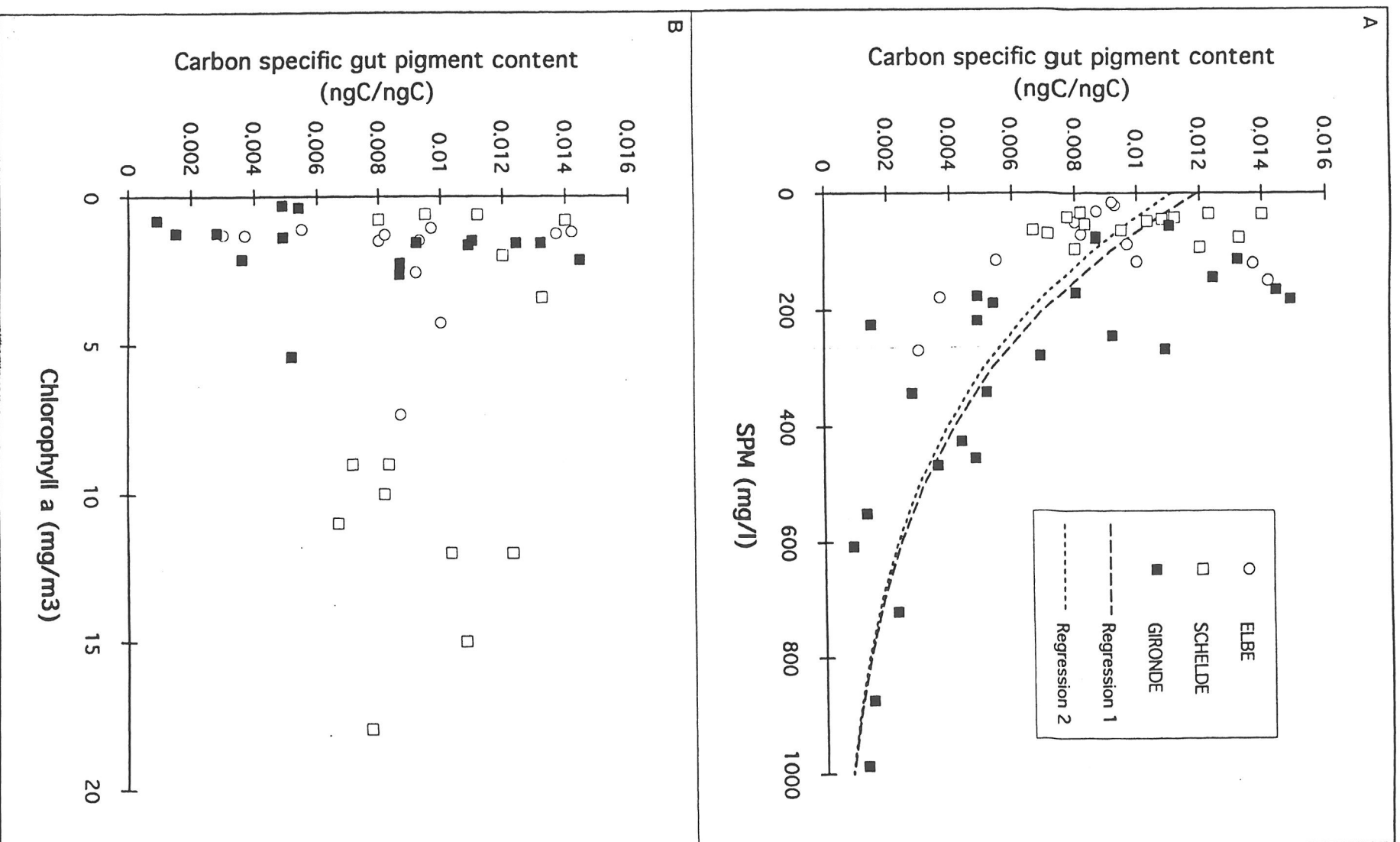


Fig. 25. Relationship between gut fluorescence of *Eurytemora affinis* and a) total suspended particulate matter (SPM) and b) chlorophyll-a concentration in the water. From: Gasparini et al., this report.

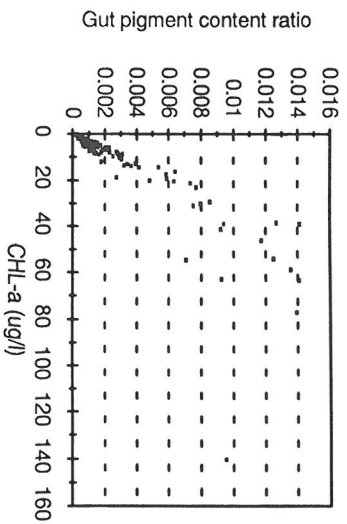


Fig. 26 a

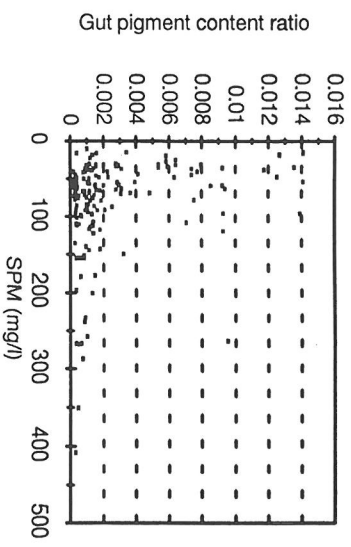


Fig. 26 b

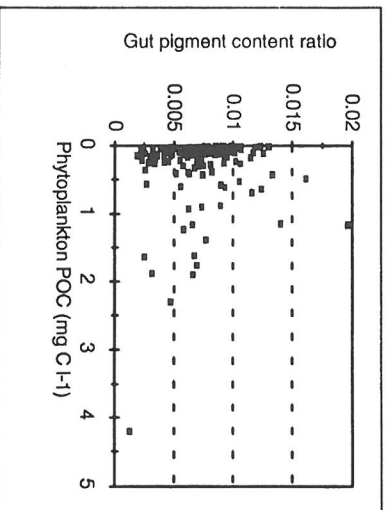


Fig. 26c

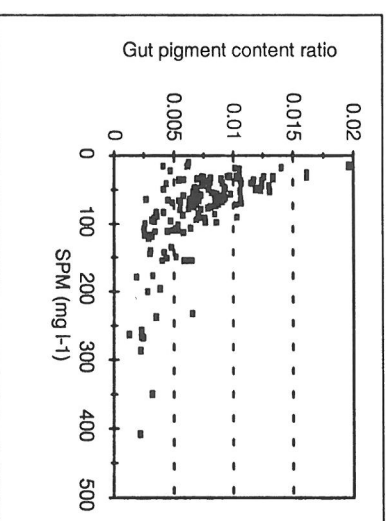


Fig. 26 d

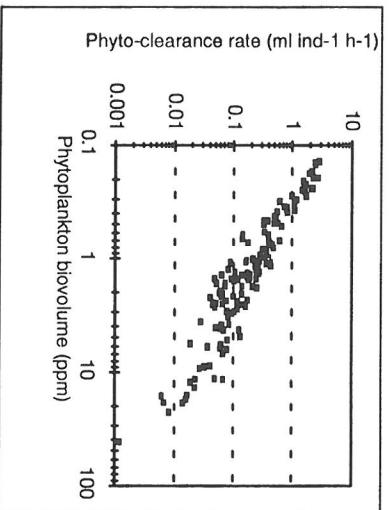


Fig. 26e

Fig. 26. Results of model calculations on selectivity by *Eurytemora affinis* for phytoplankton. a) and b) resulting gut pigment content from a model assuming no selectivity. c), d), e) results from a model assuming that chlorophyll-a uptake is proportional to the remainder of gut volume after taking up non-phytoplankton POC with a low affinity. All model results are calculated using observed values of POC, SPM and chlorophyll-a concentrations in the MATURE campaigns, thus showing their natural correlations. Details of models and parameters in the text.

List of sub-reports of the partners.

Herman, P.M.J. and B.J. de Hoop. The MATURE database.

Eisma, D. In-situ measurements of suspended matter floc size and settling velocity in the estuaries of the Elbe, Schelde and Gironde.

Brockmann, U.H., F. Edelkraut, T. Raabe, K.H. Viehweger. MATURE. Project Organic Matter and Nutrients. Final report.

Cancino, L. & R. Neves. Mature. Final report (hydrodynamical modelling).

Pfeiffer, K. Hydrographic measurements and numerical modelling contributions compiles and issued by ZMK.

Muylaert, K. & K. Sabbe. Structure and spatial distribution of spring phytoplankton assemblages in and around the maximum turbidity zone of estuaries: a comparison between the estuaries of the Elbe (Germany), the Schelde (The Netherlands/Belgium) and the Gironde (France).

Kromkamp, J., J. Peene, P. van Rijswijk, P. van Breugel & N. Goosen. A comparison of phytoplankton primary production in three turbid, European estuaries: The Elbe, Westerschelde and Gironde.

Hernandez, A., N. Raymond, J. Castel & P. Caumette. Spring distribution of bacterioplankton and production-predation relationships in the Gironde, Elbe and Schelde estuaries.

Bonin, P., N. Raymond, A. Hernandez & P. Caumette. Interaction between nitrate freshwater input, particulate organic matter and denitrification in the maximum turbidity zone in three european estuaries: Elbe, Gironde, Scheldt.

Raymond, N., A. Hernandez & P. Caumette. Sulfate reduction in estuarine sediments.

Tackx, M.L.M., R. Billones, L. Zhu, N. Daro & A. Flachier. Feeding of zooplankton on microplankton and detritus.

Irigoiien, X. and J. Castel. A simple mathematical model to estimate net primary production in the Gironde estuary.

Irigoiien, X., D. Burdloff, J. Castel & H. Etcheber. The role of the maximum turbidity zone controlling phytoplankton production and organic matter quality.

Irigoiien, X., J. Castel & S. Gasparini. Gut clearance rate as predictor of food limitation situations. Application to two estuarine copepods, *Acartia bifilosa* and *Eurytemora affinis*.

Gasparini, S., J. Castel & X. Irigoien. Egg production, growth rate and nutritional activity of the estuarine copepod *Eurytemora affinis* in the MTZ.

Gasparini, S., J. Castel & X. Irigoien. Longitudinal distribution of the copepod *Eurytemora affinis* (Poppe) in 3 european estuaries.

Fockedey, N. & J. Mees. Theme 4: Higher trophic levels, partim hyperbenthos.

Jak, R.G. & K.J.M. Kramer. Adjustment of low oxygen regimes and effects of hypoxia on an estuarine plankton community in enclosures.